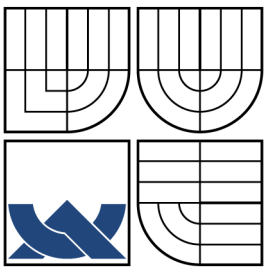

BRNO UNIVERSITY OF TECHNOLOGY
VYSOKÉ UČENÍ TECHNICKÉ V BRNĚ

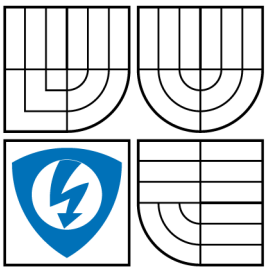

FACULTY OF ELECTRICAL ENGINEERING AND COMMUNICATION
DEPARTMENT OF CONTROL AND INSTRUMENTATION
FAKULTA ELEKTROTECHNIKY A KOMUNIKAČNÍCH TECHNOLOGIÍ
ÚSTAV AUTOMATIZACE A MĚŘICÍ TECHNIKY

CHARGE CONTROLLER FOR SOLAR PANEL BASED CHARGING OF LEAD-ACID BATTERIES

REGULÁTOR PRO NABÍJENÍ OLOVĚNÝCH AKUMULÁTORŮ Z FOTOVOLTAICKÉHO PANELU

MASTER'S THESIS
DIPLOMOVÁ PRÁCE

AUTHOR
AUTOR PRÁCE
Bc. PETER KORENČIAK

SUPERVISOR
VEDOUCÍ PRÁCE
doc. Ing. PETR FIEDLER, Ph.D.

BRNO 2011

BRNO UNIVERSITY
OF TECHNOLOGY

Faculty of Electrical Engineering and
Communication

Department of Control and Instrumentation

Diploma thesis

master's study field
Cybernetics, control and Measurements

Student: Bc. Peter Korenčiak
Year of study: 2

ID: 72963
Academic year: 2010/11

TITLE OF THESIS:

Charge controller for solar panel based charging of lead-acid batteries

INSTRUCTION:

Perform a review of methods used for and issues related to charging of lead-acid batteries. Design a concept of controller that will enable charging and discharging of number of lead-acid batteries in applications, where the source of power is photovoltaic panel. Implement the charging controller.

REFERENCE:

Using the bq2031 to Charge Lead-Acid Batteries, Unitrode Application note U-210, http://www.nalanda.nitc.ac.in/industry/appnotes/Texas/analog/slua017.pdf

Assigment deadline: 7.2.2011

Submission deadline: 23.5.2011

Head of thesis: doc. Ing. Petr Fiedler, Ph.D.
Consultant:

prof. Ing. Pavel Jura, CSc.
Subject Council chairman

WARNING:

ABSTRACT

This thesis deals with the design and implementation of a charge controller for multiple lead-acid batteries to be used in a solar system. Such controller enables an independent connection and charge control for each of more batteries with possibly different age and parameters. It is in contrast with solutions with one connection for multiple batteries connected in parallel, where mixing different battery types or ages is not recommended. This controller offers very high scalability of energy storage in solar system. It is also possible to use older batteries together with new ones instead of having to replace the old batteries when their capacity falls below required level.

The requirements, hardware and software design along with the implementation of such controller with 20A nominal output current for five 12V lead-acid batteries are discussed in detail in this thesis. Additional features, alternative designs and algorithms are discussed as well. An important part of the work concentrates on high current switch design, short circuit protection as well as circuit for DC current measurement. Correct functionality of the implemented controller has been verified by measurements.

KEYWORDS

charge controller, charging, multiple lead-acid batteries, photovoltaic panel, solar system

ABSTRAKT

Tato diplomová práce se zabývá návrhem a realizací regulátoru pro použití v solárním systému s větším počtem olověných akumulátorů. Takový regulátor umožňuje nezávislé připojení a řízení nabíjení většího počtu akumulátorů různého stáří a parametrů. To je v kontrastu s řešeními obsahujícími jedno připojení pro více baterií připojených paralelně, kde se míchání baterií různého druhu a stáří nedoporučuje. Tento regulátor nabízí vysokou škálovatelnost skladování energie v solárním systému. Umožňuje také používat starší baterie s novými, místo nutnosti staré baterie nahradit, když jejich kapacita klesne pod požadovanou úroveň.

V této práci jsou podrobně popsány požadavky, návrh hardwaru a softwaru a implementace regulátoru s nominálním výstupním proudem 20A pro pět 12V olověných baterií. Práce popisuje také další funkce, stejně jako alternativní návrhy a algoritmy. Důležitá část práce se zabývá designem spínačů pro velké proudy, ochrany proti zkratu a obvodů pro měření stejnosměrného proudu. Správná funkčnost regulátoru byla ověřena měřením.

KLÍČOVÁ SLOVA

regulátor nabíjení, nabíjení, vícero olověných akumulátorů, fotovoltaický panel, solární systém

KORENČIAK, P. *Charge controller for solar panel based charging of lead-acid batteries*. Brno: Brno University of Technology, Faculty of Electrical Engineering and Communication, 2011. 89 p. Master's thesis supervised by doc. Ing. Petr Fiedler, Ph.D.

DECLARATION

I declare that I have elaborated my master's thesis on the theme of "Charge controller for solar panel based charging of lead-acid batteries" independently, under the supervision of the master's thesis supervisor and with the use of technical literature and other sources of information which are all quoted in the thesis and detailed in the list of literature at the end of the thesis.

As the author of the master's thesis I furthermore declare that, concerning the creation of this master's thesis, I have not infringed any copyright. In particular, I have not unlawfully encroached on anyone's personal copyright and I am fully aware of the consequences in the case of breaking Regulation § 11 and the following of the Copyright Act No 121/2000 Vol., including the possible consequences of criminal law resulting from regulations in part two, chapter VI., volume 4 of Criminal Act No 40/2009 Vol.

PROHLÁŠENÍ

Prohlašuji, že svou diplomovou práci na téma „Regulátor pro nabíjení olověných akumulátorů z fotovoltaického panelu“ jsem vypracoval samostatně pod vedením vedoucího diplomové práce a s použitím odborné literatury a dalších informačních zdrojů, které jsou všechny citovány v práci a uvedeny v seznamu literatury na konci práce.

Jako autor uvedené diplomové práce dále prohlašuji, že v souvislosti s vytvořením této diplomové práce jsem neporušil autorská práva třetích osob, zejména jsem nezasáhl nedovoleným způsobem do cizích autorských práv osobnostních a jsem si plně vědom následků porušení ustanovení § 11 a následujících autorského zákona č. 121/2000 Sb., včetně možných trestněprávních důsledků vyplývajících z ustanovení části druhé, hlavy VI. díl 4 Trestního zákoníku č. 40/2009 Sb.

Brno ....

(podpis autora)

ACKNOWLEDGEMENT

I would like to express my deepest gratitude to my advisor doc. Ing. Petr Fiedler, Ph.D. for his helpful comments, suggestions and guidance throughout the work on this thesis. I thank my parents for their support during my studies and to Ing. Miloš Caha for his suggestions, designing the board layout and producing the printed circuit boards for the prototype of the charge controller.

Brno ....

(author's signature)

CONTENTS

LIST OF FIGURES

LIST OF TABLES

INTRODUCTION

First photovoltaic (PV) solar panels[1] have been designed and used mainly in space technology, as the production costs of such panels were very high. As the time passes, the photovoltaic cells can be produced cheaper and cheaper and their efficiency is rising. This is also a reason why they are being used much more frequently and it is not rare to see them on the rooftops any more. The future offers even bigger possibilities, as new thin plastic solar cells are being developed with prospects of cheap large scale production using printing technology [4].

Photovoltaic solar systems can be divided into two basic categories – *grid connected* and *off-grid* (also *stand alone* or *isolated*) solar systems. The grid connected systems feed the electricity produced by solar panels to the grid using an inverter. When the electricity is needed during night or periods with little sunlight, the energy is taken back from grid. In isolated systems, the excess electricity is usually stored in batteries during the day and batteries are used to power the appliances in times when photovoltaic panels do not produce enough energy.

Solar regulators (also known as charge controllers) play an important part in isolated solar systems. Their goal is to ensure the batteries are working in optimal conditions, mainly to prevent *overcharging* (by disconnecting solar panel when batteries are full) and too *deep discharge* (by disconnecting the load when necessary).

There are plenty of such controllers to choose from on the market, but up to author's knowledge and research none of them has more than one output for charging the battery. The aim of this master thesis is to design a solar regulator that could control more lead-acid batteries at the same time. The design is limited to lead acid batteries, as they are currently the most used type in the isolated photovoltaic applications due to their high capacity and very good price per capacity compared with other battery types.

Why would anyone want to use such controller when you can easily connect more batteries in parallel when needed? As one may know, lead-acid batteries can only be connected in parallel to increase the overall battery pack capacity when the individual batteries are of the same batch and age. The reason for this is that as the batteries get older, their parameters such as internal resistance are changing and this affects their voltage level. If a new battery is interconnected with an old one, the old battery with lower voltage levels acts as a load for the new battery which usually loses its capacity faster.

Having solar regulator that would be able to keep the individual batteries at

[1] Photovoltaic means that the primary purpose is producing electricity out of light. The term solar panel can be sometimes used also for systems designed to convert sunlight into heat, but this is not the case in this thesis.

their own independent voltage levels would have many advantages. It would enable the user to use the old battery pack with the new batteries instead of replacing the battery when the capacity of the old ones drops below useful levels. Increasing the capacity of a battery pack after some time in use would be also without problems using this charge controller. Being able to use the older (less efficient) batteries till the very end of their service life together with new (more efficient and more reliable) ones would increase the overall capacity of the battery pack and increase the performance of the solar system while ensuring safe and robust operation.

The positive economic impact of such solution is indisputable. The fact that lead acid batteries have a lifetime of about 5 years and that their price is not marginal emphasizes the possible savings even more.

This thesis will be divided into several fundamental blocks. The optimal charging of lead-acid batteries, the intended functionality of the controller, block diagrams and the subsequent design requirements will be discussed in the first chapter called Requirements. The chapters Hardware design and Software design will discuss specific design possibilities considered and choices made in respective parts. Last chapter will present the measurements performed on the implemented prototype of charger controller.

1 REQUIREMENTS

The main purpose of this thesis is to produce a prototype of charge controller (solar regulator) that could control multiple lead-acid batteries at the same time. It is to be applied on 12V batteries, because this voltage is most commonly used in isolated solar systems. The reason is that there are a lot of appliances for cars (which usually use 12V batteries) that can be easily used instead of more expensive ones designed for non-standard voltage.

The background about lead-acid batteries and their charging will be mentioned in the following section, as this is the basis for designing a useful solar regulator.

1.1 Lead-Acid Batteries

"A lead-acid battery is a electrical storage device that uses a reversible chemical reaction to store energy. It uses a combination of lead plates or grids and an electrolyte consisting of a diluted sulphuric acid to convert electrical energy into potential chemical energy and back again" [39].

1.1.1 Background

Before an initial charge, the lead electrodes of lead-acid batteries are both the same and the electrolyte is sulphuric acid. When they are initially charged, the cathode is oxidized into lead (II) oxide, while the anode remains unchanged.

Subsequent discharging changes both electrodes to lead sulfate and the sulfuric acid is diluted. Recharging simply restores the previous state (the electrodes return to lead and lead oxides). [5]

When the batteries are overcharged (charged even after most of the sulfate has been converted), the excess energy is used to split the water in the electrolyte into hydrogen and oxygen gases.

A battery "capacity, C, refers to the number of ampere-hours that a charged battery is rated to supply at a given discharge rate. A battery's rated capacity is generally used as the unit for expressing charge and discharge current rates, i.e., a 2.5 amp-hour battery charging at 500mA is said to be charging at a C/5 rate" [40].

1.1.2 Types

Lead-acid batteries can be divided according two basic criteria – purpose and construction. According to purpose they are divided into [39], [5]:

Starter batteries – their purpose is to start the engines in cars, so they are made so that they can supply very high currents. However, they are not suitable to be deeply discharged, as they have thinner electrodes that are more susceptible to mechanical stress arising from cycling.

Deep cycle batteries – these batteries tolerate the deep discharges much better thanks to thicker plates.

According to construction, the batteries are divided into:

Flooded – the type, where the gases and vapours are allowed to escape from the container. In some of them the lost water can be replenished.

Valve regulated lead-acid (VRLA) – "VRLA batteries remain under constant pressure of 1-4 psi. This pressure helps the recombination process under which 99+% of the Hydrogen and Oxygen generated during charging are turned back into water. The two most common VRLA batteries used today are the Gel and Absorbed Glass Mat (AGM) variety" [39].

1.1.3 Issues

The lead-acid batteries experience several phenomenons, that affect their performance [5]:

Self-discharge – this is common to all battery types, not only lead-acid.

Gassing – happens when batteries are overcharged and it is caused by hydrolysis of water from the electrolyte into hydrogen and oxygen.

Sulfation – refers to crystallization of lead sulfate that is released on the plates when the battery is discharged. When in crystalline form, it cannot take part in the chemical reaction and effectively blocks the access of electrolyte to electrodes. It causes the battery capacity to drop over time and it is accelerated by leaving the battery in an uncharged state. According to sources of [5], it is possible to prevent or hinder this process "by a desulfation technique called pulse conditioning, in which short but powerful current surges are repeatedly sent through the damaged battery. Over time, this procedure tends to break down and dissolve the sulfate crystals, restoring some capacity."

Stratification – this term refers to division of electrolyte into layers with different concentrations of the electrolyte due to different density of water and sulfuric acid. This "can lead to greater corrosion of the bottom half of the plates" [5]. It is prevented when the battery is frequently in motion (such as in car) or by gassing, where the gas bubbles stir the electrolyte when moving through it.

Freezing – the electrolyte can freeze, especially when the battery is discharged when it contains more water (added by the chemical reaction during discharging). The freezing point therefore depends on a state of charge of battery.

Freezing can mechanically damage the battery.

Dehydration – happens when the flooded battery loses water due to overcharging. The water has to be replenished, so that the electrodes do not dry up. Therefore it is not desirable to overcharge flooded batteries significantly.

1.1.4 Charging

The issues listed in the previous chapter can be avoided when adhering to very simple basic rules for charging the lead-acid batteries (the voltages mentioned are valid for 6 cell, 12V batteries [5]):

- disconnect the load when the battery voltage decreases below typically 10.5V when loaded,
- it is possible to charge the battery indefinitely (*float charging* or also called *preservation charging*), if its voltage is kept below certain threshold (varies according to battery type between 13.4 and 13.8V),
- when cycled (going through charging and discharging phases consecutively), the battery termination voltages are higher than when charging indefinitely (14.2 to 14.5V),
- it is not good to charge battery beyond the gassing voltage (about 14.4V) for longer periods of time,
- it is good to change the voltage levels according to battery temperature, as the voltage values have a significant temperature characteristics,
- it is safe to charge most of lead-acid batteries by currents up to C/10h, where C is the battery capacity in Ah.

However, the ideal charging of lead-acid batteries consists (according to sources [41], [40]) of three stages: *constant-current charge*, *topping charge* and *float charge*. Battery voltage and current levels per cell during these stages are illustrated in Fig. 1.1.

Most of the energy is transferred to the battery during the first stage. The second stage overcharges the battery a little while the current decreases. This is important to recharge battery to 100% of its previous capacity. The losses due to self-discharge are compensated during the last stage.

The charge controller can be devised in several stages, so that the simple guidelines for charging are met in the prototype stage. After this functionality is implemented and verified, the algorithms to achieve ideal charging (described above) can be implemented to improve the quality of charging process.

From the basic guidelines it is clear, that the minimum functionality that the hardware of the controller has to implement is voltage measurement and switching off the load and input from solar panel.

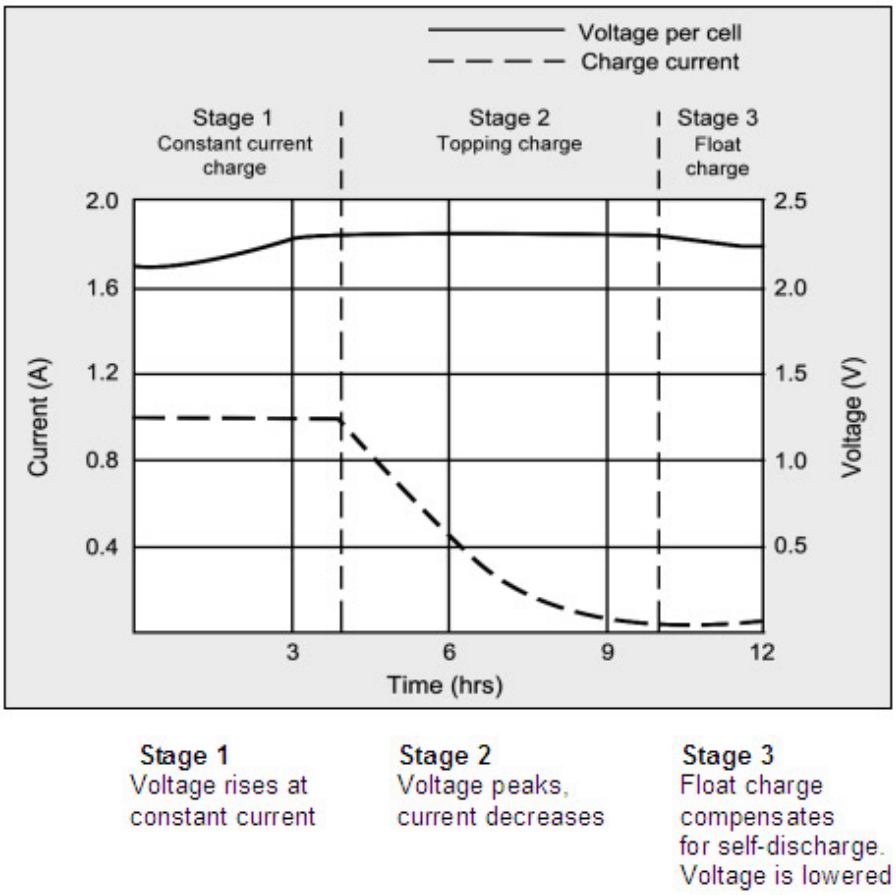

Fig. 1.1: The diagram of charging stages of lead-acid battery [41]

Further requirements have however not been specified in the assignment of this master thesis. So in order to guarantee a sensible design that could possibly compete with other available solar regulators the list of features considered to be ideal for this controller has been put together in the next section.

1.2 Considered Functionality

Except for standard features (overcharge protection, low voltage disconnect) of solar regulator, the following functionality would be ideal for solar regulator:

1. **Multiple high current terminals for connecting batteries** – the terminals and all other power electronics should be able to withstand at least 20A of current at nominal voltage of 12V. This value should be high enough for most practical applications on 12V system, since the controller would be able to deliver 240W of power to the load and charge the batteries with the same amount of power. Being able to deliver higher currents would be useless for most practical applications, since the resistance of cables would become an

issue. It is assumed that if user requires more power to be delivered from the solar system, he will use systems with higher nominal voltage (24V or higher).

2. **Input and output power measurement and logging** – this capability is the basis for using many of the below-mentioned functions. It requires measuring the instantaneous current and voltage on each battery. Using this data, the power flowing to and from the battery could be calculated.
3. **Battery performance analysis** – an algorithm for analyzing the data logged from the power measurements could be implemented. This could calculate the efficiency of energy storage in each battery and compare the quality of installed batteries over time. Such algorithm could easily identify the end of useful life of individual batteries and the need for their replacement.
4. **Condition monitoring and display** – the measurements of supplied and received energy of the whole battery pack could be used to estimate the remaining energy in storage. This and the data from the instantaneous measurements (of current and voltage) could be presented to the user using Liquid Crystal Display (LCD).
5. **Over-current protection** – as the charge controller will be designed to withstand some specific maximum value of continuous current, surpassing this value could lead to damage of regulator as well as batteries due to excessive generation of heat. The over-current condition should be monitored and the load disconnected, should this condition last for longer periods of time.
6. **Short circuit protection** – even though short circuit condition can be thought of as an over-current condition, special care has to be taken in this case. The main objective is to protect the semiconductor switches (that will most probably be used) from instantaneous large spikes of current that occur during short circuit. The reason is that semiconductor switches are very susceptible to damage from such condition, even if it takes only short periods of time and no other effects (especially thermal) can be observed. That is why the protection will have to be designed to be quick enough to protect these devices.
7. **Interface for connection to PC** – this functionality would be useful if data logging functionality is implemented to download measured data to PC using RS232 or USB port. The user could for example analyze the data of daily electricity usage and production and make informed decisions about any system modifications (such as addition of solar panels, batteries, complementary sources of power for periods when solar energy output is not sufficient).
8. **Reverse battery connection protection** – it is not needed for normal operation, but this feature would protect the device from improbable but otherwise very dangerous mistake when connecting the device to other components of solar system.

9. **Thermal protection** – this functionality is considered to be implemented in case the power dissipation of the power switches is higher than the implemented cooling can dissipate. The reason is that in the prototyping phase one can not be sure of the exact operating conditions (temperature range) and possible problems that may arise during operation. Temperature sensing on the most thermally stressed components (or on their heat sinks) and over temperature shutdown would ensure the device is operating safely under any conditions.
10. **Battery temperature measurement** – since the electrical characteristics of batteries are temperature dependent, the charging currents and conditions could be adjusted to instantaneous battery temperature to improve the overall charging performance and prolong the battery lifetime. The implementation may require a separate temperature sensor to be connected to controller so that the temperature can be detected as close to batteries as possible.

Implementing these features or at least making the system expandable with these advanced features or algorithms would be great advantage in the future. It would make the final product competitive with other solar regulators.

There are also features that have been considered, but are *not intended* to be implemented in the charge controller:

1. **Input for external power supply** – this feature could be useful for applications, where analysis of electricity production from solar panel would be required feature. It would enable differentiation of supplied current from solar panel and external source of power that could be used during longer periods without enough sunshine for the solar panels to produce enough energy. An output of a diesel generator, wind turbine or any other source of power would be needed to recharge the batteries. This feature is not intended to be implemented, as the added costs and complexity (due to additional HW requirements) are higher than the possible benefits that are limited only to few users, who would care about the detailed performance analysis. The reason is that when needed, external source of power for recharging batteries can be easily used in parallel with solar panel, if both this source and solar panel are each connected through a simple diode that would prevent the current flowing into the solar panel.
2. **Peak power tracking** – special controllers use this technology to maximize the power output from the solar panel. It is based on DC/DC converter that adjusts its power throughput so that the solar panel works at its maximum power point (the maximum power point of solar panel varies with momentary temperature and illumination). Several methods for maximum power peak tracking have been designed and implemented, e.g. a solution described in [8]. One of the most important parts of peak power tracking controller is current

and voltage sensing. As the proposed controller should implement this feature, peak power tracking capability was considered to be implemented as well. However, due to potential problems, bigger complexity, the fact that peak power tracking controllers are commercially available, and because they can be used in series with the regular solar regulators, plans for implementing this feature have been abandoned.

3. **Current limiting** – This ability would be useful to limit the charging current for batteries with small nominal capacity to C/10 or other value that would be suitable for the battery. Instead of implementing this feature, it is expected that the user pairs the power of the solar panel with the appropriate battery sizes. Alternatively, if the maximum current from the photovoltaic panel is higher than the maximum allowed charging current for the batteries, the user will be advised to put the batteries of the same batch and age in parallel to ensure the maximum charging current condition for each battery is met. The main reason for not implementing this feature is the fact that in most systems the battery sizes are high enough. Therefore the probability of occurrence of this problem is low. Furthermore the added concerns for the user would be similar with or without this feature, as he would have to manually enter the battery capacity value (or maximum charging current) for every battery even if it was implemented.

After the desired features of the product have been defined, it is possible to create a block diagram that could roughly implement most of the features.

1.3 Block Diagram

Based on the intended functionality mentioned in the previous chapter, the preliminary block diagram of the charge controller in Fig.1.2 has been devised.

1.3.1 Preliminary Block Diagram

The exact number of batteries is not indicated in the Fig.1.2, as it is not defined yet. It will be determined according to hardware design possibilities that will be clearer at a later stage. It will mostly depend on the added cost and complexity of hardware and the design will aim to make this number as high as is practical.

The regulator built according to this block diagram will have capability to measure the voltages of all batteries. These measurements can be used by the microcontroller (µC) to control the inputs from solar panel to each battery separately and the outputs to load in the same way. So the controller will have possibility to stop

charging, when the battery is fully charged as well as disconnect the load, when it is fully discharged.

The diagram contains also some optional blocks that may not be implemented in final version. However, these have been included in order to show the configuration of blocks if all of the desired functionality is implemented.

1.3.2 Updated Block Diagram

The block diagram in Fig. 1.2 has been used throughout most of the design phase, because the switches were assumed to be unidirectional. However, later it was discovered that it can be simplified.

The simplification is based upon using only one common path for currents from solar panel to batteries and from batteries to load, as shown in Fig. 1.3. This was possible after a specific design of power switches done in Section 2.1.1 was changed so that the switches were made bidirectional.

In order to ensure that the regulator can perform charging correctly, two more switches had to be added. Namely a switch that can disconnect a solar panel and a switch to disconnect load, when all of the batteries on the common bus are fully charged or discharged. The regulator will of course be able to choose which battery will be connected to the bus. This way all the major objectives can be fulfilled.

For more details about the design of power switches, reasons for making the change and the details about the simplification please refer to Section 2.1.1.

The preliminary block diagram has set a basic shape for the controller design that could lead to fulfilment of highest level requirements as well as created logical sub-blocks. For these blocks, separate detailed requirements can be made.

1.4 Definition of Design Requirements for Building Blocks

The elements of the block diagrams from the previous section should ideally have following characteristics:

LCD – for displaying information about battery and controller state and measured data. The display may need to be switched on only for short periods of time after any key is pressed due to power saving reasons.

LEDs – two low power consumption LEDs (red and green) for indication of correct function or any error when LCD is switched off.

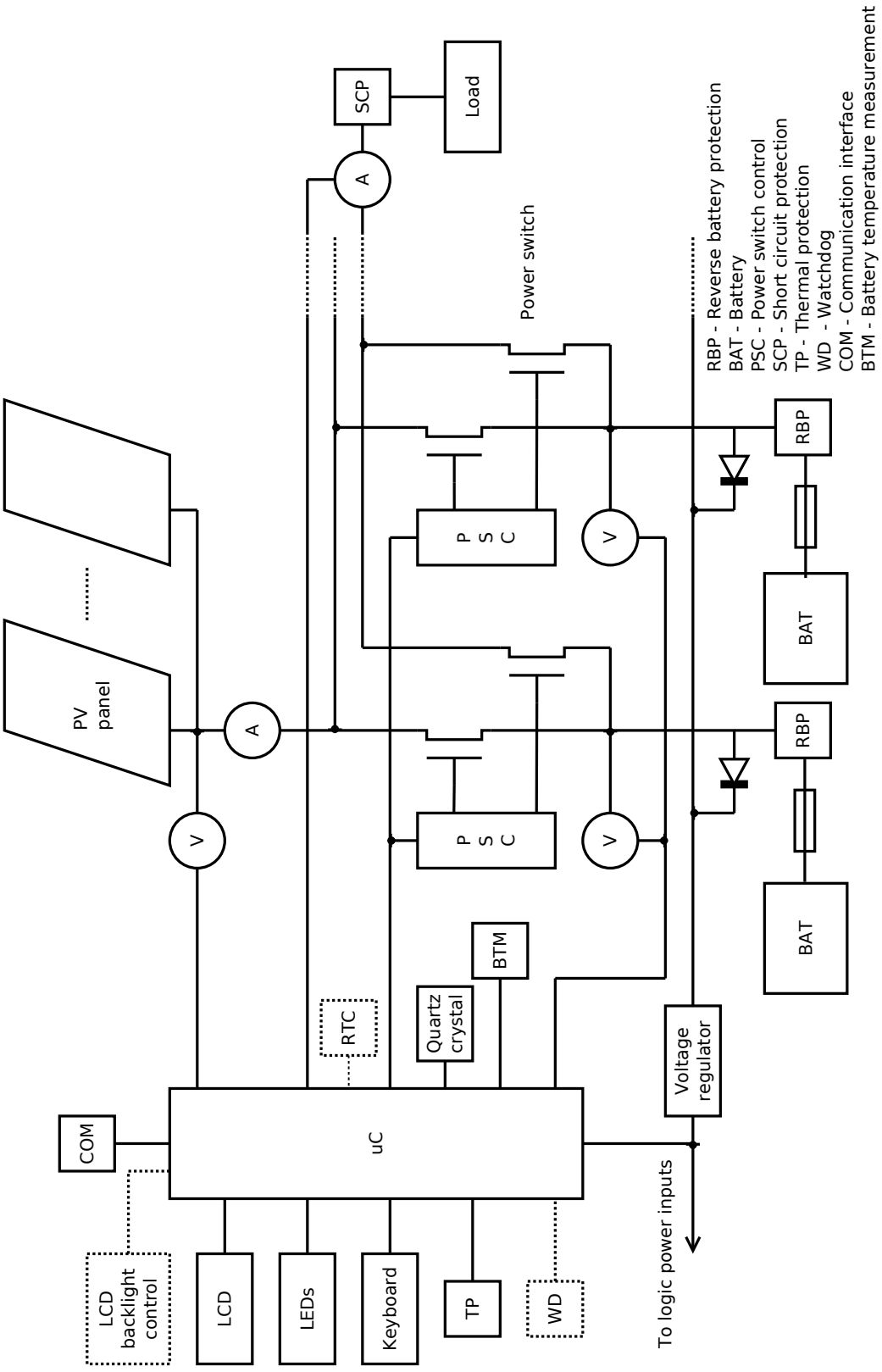

Fig. 1.2: Preliminary block diagram of solar charge controller

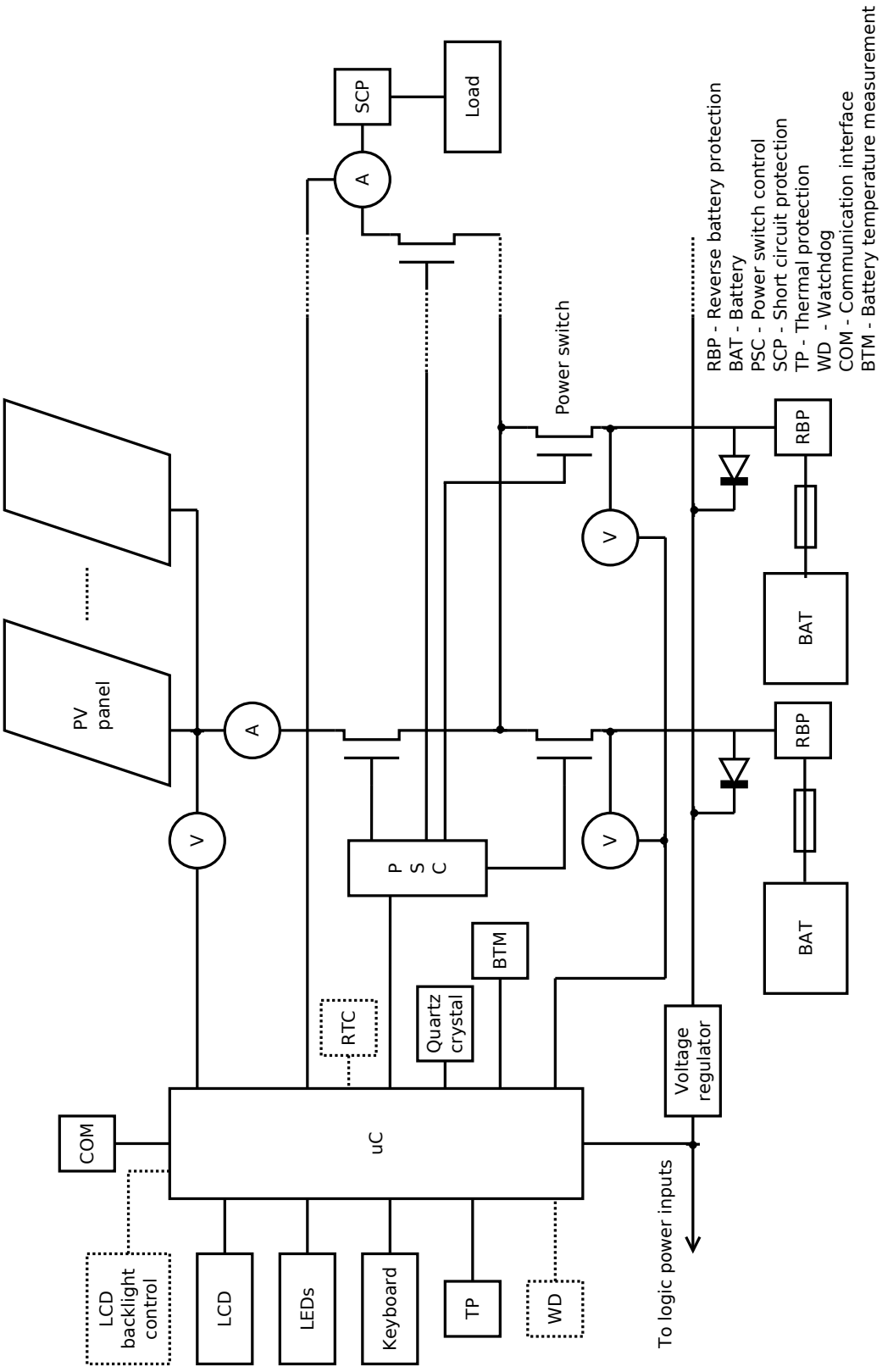

Fig. 1.3: Updated block diagram of solar charge controller

Keyboard – for controlling regulators' functionality and setting parameters. Only three keys (*up*, *down* and *enter*) should be needed, if sophisticated menu is implemented.

Thermal protection – a temperature sensor capable of measuring temperatures in the range from -30 to about +160°C.

Battery temperature measurement – a temperature sensor capable of measuring temperatures in the range from -30 to about +50°C.

External watchdog (optional) – should restart a µC after specified time interval (between 150 and 1200ms) and after a power failure.

Voltage regulator – will have to be chosen according to sum of maximum consumption of active components such as µC that it will feed power to.

Reverse battery protection – has to be able to withstand voltage of about 30V and prevent damage of controller and/or batteries.

Short circuit protection – should disconnect the load when it is shorted. Its parameters depend on the kind of switches used, as this is mainly for their protection. It also has to have least possible series resistance.

Power switch control – should convert voltages that will be an output of the µC to levels that are large enough for power switches used.

Battery – a lead-acid battery with nominal voltage of 12V.

Serial communication interface – to be able to communicate with a PC or to decompose the regulator into more parts (e.g. main part and a user interface module and/or datalogging module).

Voltmeter by the PV panel – should be able to withstand voltages in range of 0 to +25V (as the PV panel nominal voltage of 12V generates about 24V when load is disconnected).

Voltmeters by the batteries – should work in range of 0 to +15V.

Ammeter – the measuring range should be 0 to little over 20A to be able to detect over-current condition.

Power switch – should be able to handle currents of 20A or higher (ideally at least 30A so that there is some reserve) and withstand voltages of 30V or higher. Very low series resistance is also a must.

LCD backlight control – should be able to switch the currents needed by backlight of the LCD module according to a logic signal on one pin of the µC. The backlight should ideally be switched off after about 15s from pressing one of the keys last time in order to decrease the overall power consumption of the device.

Quartz crystal resonator – for the internal clock signal generator of µC. Its value should be considered according to computational power requirements of algorithms used and the power consumption of the µC. Currently 2MHz value

is considered to be a good compromise.

Microcontroller – needed as most of the planned functionality of charge controller requires use of digital electronics for implementation. The µC should have enough pins for at least the mandatory features (if µC with fewer pins is selected, some of the optional functionality may not be implemented). As the exact memory requirement will not probably be known until most of the algorithms are actually developed, µC with more built in memory should be preferred (even if not used by algorithms, it can be utilized for logging purposes). The µC may have internal Analog to Digital Converter (ADC) to save an extra part, but in this case must have enough inputs for it.

Real-Time Clock (optional) – using it for timekeeping instead of counting the time in the microcontrollers main loop will allow the µC to sleep when no other tasks need to be calculated, thus saving power.

When the design requirements for all of the individual building blocks have been specified, it is possible to carry out the design by these requirements itself, as is done in the following chapter.

2 HARDWARE DESIGN

This chapter concentrates on all aspects of hardware (HW) design of the controller, such as the realization of individual building blocks, issues connected to interconnection of these blocks, producing the Printed Circuit Board (PCB) and prototype of the regulator.

2.1 Design of Fundamental Building Blocks

There are three stages of designing this block that have been labelled as the first design, second design and the third (and final) design. After encountering problems that will be specified later, the original conceptual solution (first design) has been redesigned. Later was found that the second design can be substantially simplified with little or no effect on functionality.

The biggest difference between the first two designs is that the first design relied on using the positive terminals of the batteries as 0V and was supposed to work with negative voltages. This idea has been abandoned later and the second design uses the minus pole as a common reference and works with positive voltages. The reason for this change will be explained in detail in paragraph Second design (Section 2.1.1).

The siplifications that lead to the third design deal mainly with the power switching and do not impact other building blocks very much. More details will be discussed in paragraph Third design (Section 2.1.1).

2.1.1 Power Switch and Power Switch Control

As the power switches are probably the most important parts of the proposed regulator, their design is considered first. Their significance is due to fact there are more of them and also because they have the biggest impact on the final performance.

Switching Technology Selection

Following technologies have been considered as a possible building block for individual switching element:

- relay,
- Solid State Relay (SSR),
- bipolar transistor, and
- Metal-Oxide-Semiconductor Field-Effect Transistor (MOSFET).

The relays have an advantage that they behave like an ideal switch – infinite resistance in open position and very little resistance in closed state. Among the disadvantages are their size and the fact that they are electromechanical devices

so they may be more prone to failure after some time. They are also quite slow compared to bipolar and unipolar transistors, so they can hardly be used for Pulse-Width Modulation (PWM).

Solid State Relays have fewer disadvantages than usual relays thanks to no mechanical components, but they are not suitable for DC switching application. The commercially available SSRs suitable for high enough currents actually contain triacs. Besides this, the devices that can handle 20A or more continuously cost about 11 times more than MOSFET transistors for comparable currents.

Bipolar transistors have an obvious disadvantage of a voltage drop equivalent to a diode drop (so about 0.6V) on them even if closed. This would result in huge power losses if currents as high as proposed nominal current of 20A flew through them. In such case the transistor would dissipate 12W of power (in reality even more, because the voltage drop over the transistor would be bigger with current of 20A, which is the highest nominal current that this regulator will be designed for).

The MOSFETs are currently capable of switching more than one hundred Amperes continuously (for example transistor IRFP064N made by International Rectifier can withstand 110A continuously with proper cooling) have a static drain-to-source on-resistance ($R_{DS(on)}$) as low as 5mΩ. What is more, the prices are competitive with any of the above-mentioned technologies. They come in two flavors: N-channel and P-channel. The N-channel transistors usually have better performance characteristics (lower $R_{DS(on)}$, able to switch higher currents) and lower price than P-channel transistors. However, they have one big disadvantage: The only simple way of connecting them in the circuit requires that the terminal that is switched is negative.

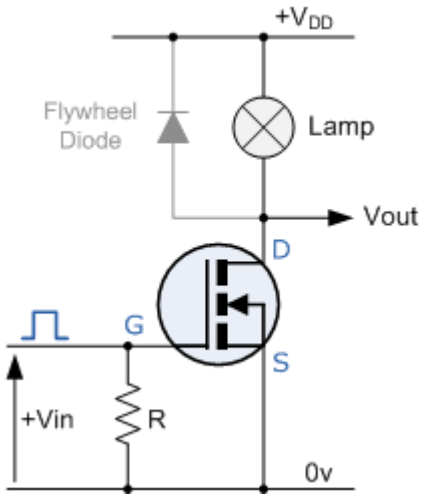

Fig. 2.1: An example of a using MOSFET as a switch [9]

The situation and the reason for this can be illustrated on diagram in Fig. 2.1. The MOSFET is turned on by a positive voltage applied between Gate and Source

terminals. This voltage can be taken directly from V_{DD} if it is less than 20V, otherwise the voltage divider has to be used. Note that the Source is placed at 0V in this case, so the voltage to turn on the transistor can be related to 0V. If the transistor was placed between the V_{DD} and lamp, the voltage to turn the transistor on would have to be applied between Gate and Source terminal and it would have to be more positive than V_{DD}. Another problem is that the Source would not have a defined potential, because that depends on the current flowing through the lamp. That is why N-channel MOSFETs are usually used in circuits such as in Fig. 2.1.

After considering all these facts, N-channel MOSFETs have been chosen as the most suitable switching technology. The reason is mainly that using this technology PWM switching will be possible if needed and the power losses can be kept as low as possible.

But this decision comes at a cost of adding complexity to the design. As was already mentioned, there is a problem with switching the positive poles with the N-channel MOSFET switches. To overcome this problem, the two approaches can be used:

1. connecting MOSFETs so that they disconnect negative poles of batteries. As a result the positive terminals will have to be used as common poles (or 0V) instead of negative terminals, as is normal under usual conditions. The negative voltages will have to be used, which means more complicated design of voltage regulation for logic and more complicated voltage measurement, as ADCs work with positive voltages only. This approach was used in the first design that will be described in the next chapter.
2. placing MOSFETs in the positive branches (and using negative poles of batteries as a common terminal) and generating a higher voltage for the gate-to-source voltage (V_{GS}) than the voltage to be switched. This will require some switching power supply or charge pump that could create higher voltage than the 12V nominal voltage that is already present in the system. There will also be problems with the gate potential floating. However, designing other subsystems (e.g. current measurement, ADC, etc.) will be easier due to having negative pole as a ground. This was later used in the Second design (Section 2.1.1).

After a preliminary selection a concrete type of MOSFET transistor has been selected: IRF3205 produced by International Rectifier. This transistor can handle drain-to-source voltage (V_{DSS}) up to 55V, continuous drain current (I_D) of 110A, its $R_{DS(on)}$ is equal to 8.0mΩ and it comes in TO220A package [17]. It is readily available in retail stores for prices of about 0.8 Euro.

This transistor clearly suffices our maximum current requirement and has also low enough $R_{DS(on)}$ value. It is a good compromise between quality and price.

However, if the price of MOSFETs with better quality drops to an adequate level, it can easily be replaced as most power MOSFETs are produced in TO220A package as well.

First Circuit Design

This is the design, where the positive terminals are used as common poles.

In the very beginning, there was only one transistor planned in one branch to be switched. After a test on the real circuit it is clear, that such design is not satisfactory. The reason is the MOSFET's body diode in the reverse direction. With this diode, the MOSFET can be used as a unidirectional switch only. If the voltage is applied in the reverse direction, the transistor conducts current as soon as the voltage reaches threshold level for diode conduction (about 0.6V).

The problem is that for successful isolation of the batteries from each other a bidirectional switch is needed (the current can not flow in any direction when the switch is open). Two solutions for this situation have been thought of:

- using a diode in series of the MOSFET, and
- using another MOSFET in opposite direction.

If the diode was used, the power losses would increase dramatically, since power would be lost due to a relatively high voltage drop on the diode. On the contrary, with using another MOSFET, the power loss would be smaller, because of the low $R_{DS(on)}$ value of MOSFETs used. At currents equal to 20A MOSFET would dissipate power equal to

$$P_{\text{MOSFET}} = V \cdot I = R_{DS(on)} \cdot I^2 = 0.008 \cdot 20^2 = 3.2\text{W} \tag{2.1}$$

whereas diode would dissipate

$$P_{\text{diode}} = V \cdot I = 0.6 \cdot 20^2 = 12\text{W} \tag{2.2}$$

Of course the less power hungry solution was selected, even though it is still not ideal, because the power losses on the switch will be effectively doubled.

When used in practice, the second MOSFET has to be switched on together with the first one. Otherwise the current would flow through the body diode. That would result in the same heat dissipation as calculated in formula 2.2.

The bidirectional design of the power switch can be seen in Fig. 2.2. Note that the displayed types of transistors Q1, Q2, Q5 and Q6 are not correct and should be IRF3205. In this case it makes no difference, since the symbol and package of the two types of transistors are the same.

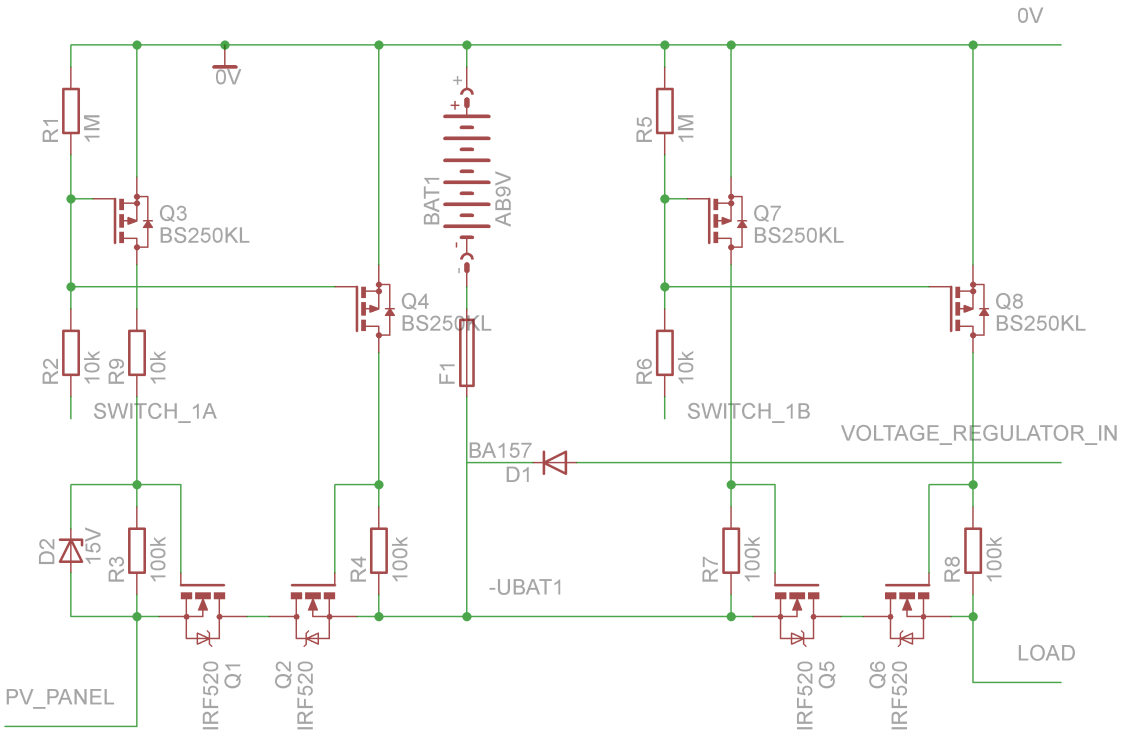

Fig. 2.2: Scheme of power switches for one battery

Theory of Operation The transistors Q1 and Q2 in Fig. 2.2 make up a pair that connects or disconnects the supply from the PV panel to battery (BAT1). As they are turned on by positive voltage applied between their Drain and Source terminals the transistors Q3 and Q4 with the resistors R3 and R4 have to be used.

The source of the Q2 is connected to –UBAT1, which means the transistor is open when its gate is at potential of –UBAT1 (or lower) and closed when the gate is at potential of –UBAT+5V or higher (up to –UBAT+20V). The Q4 with R4 actually convert the voltage levels of 0 and -5 volts from microcontroller applied to SWITCH_1A wire into either –UBAT or almost 0V (this was inspired by an example in [1]). Transistor Q4 is a P-channel MOSFET, so in this position (when source is at 0V) is turned on by -5V. When Q4 is off, there is no current flowing through R4, so the voltage between Q2's gate and source is 0V and Q2 is closed. On the other hand, if Q4 is open, there is a voltage of almost UBAT on the R4 due to current flowing which in turn turns on Q2.

The same logic applies in case of Q1 and Q3. The only difference is that there is a Zener diode D2 and a resistor R9 added. They serve as a protection against overvoltage from PV panel that could happen because PV panel for nominal voltage of 12V can generate up to 25V when no load is connected. The MOSFETs can only handle V_{GS} up to 20V, so this voltage could damage the Q1. The overvoltage

protection can be applied directly at the input from PV panel. That way the D2 and R9 and their counterparts in switching circuitry for other batteries can be omitted.

Q5 and Q6 switch the output from the battery to load according to logic signal from µC applied at SWITCH_1B. The VOLTAGE_REGULATOR_IN output feeds should be connected to voltage regulator that will power the microcontroller and other logic.

In this configuration the block in Fig. 2.2 can be used for any number of batteries and the VOLTAGE_REGULATOR_IN, PV_PANEL and LOAD wires outputs can be connected in parallel. This way only logic levels on SWITCH_nA or SWITCH_nB inputs will decide which battery is connected to solar panel and/or to load.

Drawbacks The biggest problem with this approach lies in voltage and current measurement. Mainly it is the issue of powering the ADC and what potential to use as a ground potential.

The ADC could be connected with its VCC terminal directly to 0V and -5V could be generated by 7905 circuit, which references its output to positive terminal. The problem is that the ground for ADC generated this way changes a little, because the load regulation on 7905 circuit can't be perfect. This would add another error to measurement, as all the measured voltages will be referenced to 0V and not to -5V.

This problem could be eliminated by using the 0V as a ground for ADC and powering it by +5V generated by some external circuit. This solution requires a more complicated component (power source), but does not solve the problem with grounds in current measurement, for which a specialized circuit will be used (current measurement will be discussed in subsequent chapter).

As a workaround for the abovementioned issues in this first design could not be found, a second design has been proposed.

Second Design

As was already mentioned, in this design the negative terminals of all batteries will be connected and this will be treated as 0V. The plus poles of the batteries will be switched. This can be seen on a schematic of a switching circuit for one battery in Fig. 2.3.

The plus pole of the battery will be connected to board via connector labeled as J4. The connector for the negative pole is not drawn in the picture, but it will be connected to 0V elsewhere.

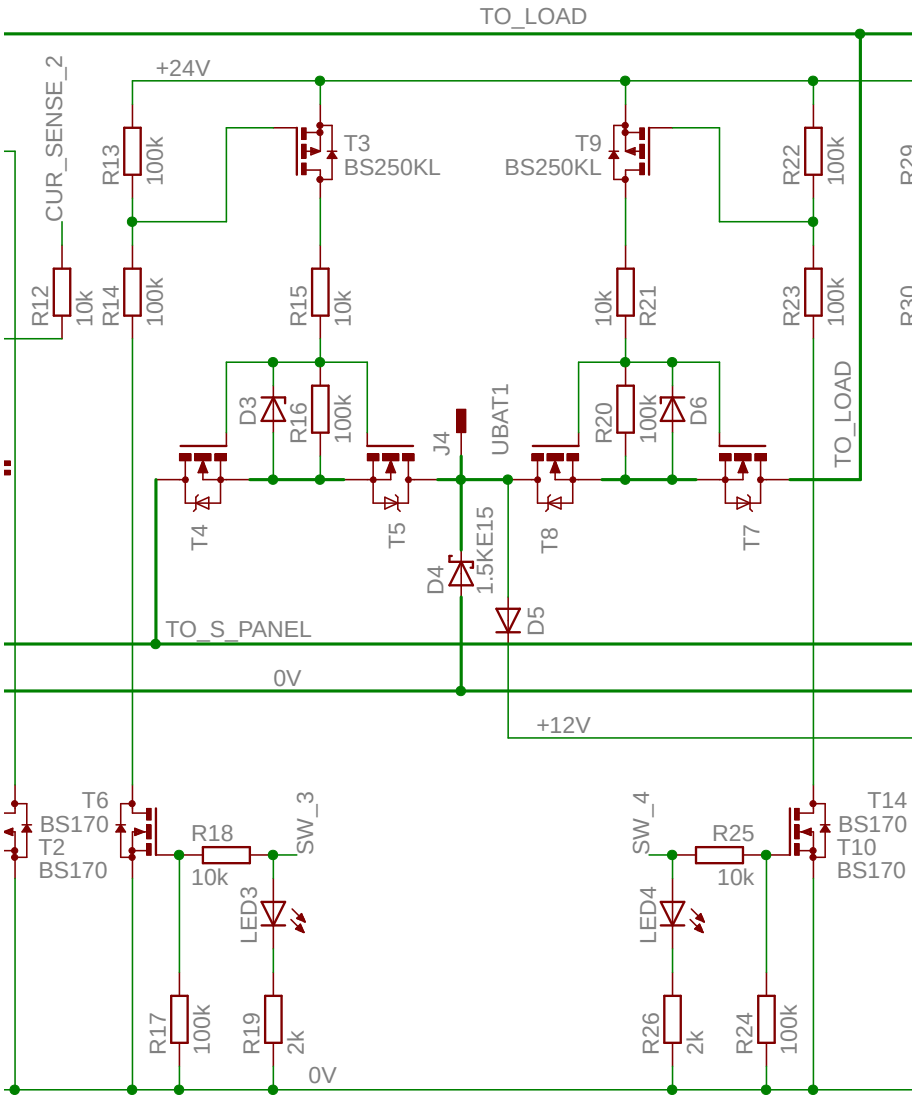

Fig. 2.3: The schematic of a power switch for one battery – second design

There are again two MOSFETs in each switched branch (to solar panel and to load). However, another improvement against first design is that the source terminals of both transistors are connected together, instead of drain terminals. This allows one driving voltage to be applied to both transistors as V_{GS}. This voltage is created on R16 and R20 when transistors T3 and T9 are turned on.

In order to create positive V_{GS}, the transistors T3 and T9 have to switch more positive voltage than what UBAT1 is. The reason is that the sources of the power transistors now sit on a potential UBAT1+0.7 which is the voltage drop created on the body diode of T5 for example.

As the power transistors are fully open at VGS of about 10V and the maximum battery voltage when charging should be about 14.1V, the source of about +24V

has been chosen for powering the auxiliary transistors T3 and T9. The way +24V is generated is described in Section 2.2.3.

Several elements had to be added for the protection of the power MOSFETs, namely resistors R15, R21 and Zener diodes D3 and D6 in the Fig. 2.3. The reason is that the transistors could get damaged by excessive V_{GS}. The absolute maximum value the transistors can withstand is $\pm 20V$. This threshold could be exceeded if there was no battery connected to J4 and the load was connected to the output of the regulator. In this situation the load would in fact connect the TO_LOAD line to 0V. In this case the sources of T7 and T8 would sit on the potential of 0.7V. If the T9 was opened in this situation, the V_{GS} would be almost +24V. The situation gets worse as the voltage on the +24V line can reach +27V. This overvoltage would definitely lead to destruction of the power transistors.

Although it seems that the protection is required only on a switch between battery and load, it is not true. The same thing could happen to transistors T4 and T5 if the switch to load would be closed in the previous situation.

The risk of damaging the power MOSFETs can be avoided by using Zener diodes D3 and D6 with a Zener voltage lower than +20V limit under the highest load condition on these diodes. In order to limit the current through them, the resistors R15 and R21 are used.

For this application the current limiting resistors R15 and R21 with nominal value 10k and diodes with Zener voltage equal to 16V have been chosen. The resistors should limit the current at worst conditions to:

$$\mathrm{I_{max}} = \frac{\mathrm{V_{+24Vmax}} - \mathrm{V_{Zener}}}{\mathrm{R}} = \frac{27 - 16}{10^4} = 1.1\mathrm{mA} \tag{2.3}$$

This current is low enough not to cause thermal problems with diode or resistor and low enough for the dynamic resistance of Zener diodes to have no impact on functionality of the protection (the Zener voltage of the diode selected loaded with 5mA should be in the range of 15.3-17.1V which is well below the dangerous threshold for V_{GS}).

Finally the transistors T6 and T10 together with resistors R13, R14, R22, R23 are used for the translation of the driving voltage from logic (0-5V) to appropriate levels for T3 and T9.

The rest of the parts are used because of integration of a power switch for single battery to the whole system and the details will be discussed in Section 2.2.2.

In order to verify the functionality of this switch a temporary test circuit on development board has been prepared and the correct performance was verified. The picture in Fig. 2.4 shows switch for switching one branch (from battery to load) for one battery (top, from left to center), the source of +24V (top right) and the current

measurement circuit (on an aluminium heat sink), whose correct functionality was also verified.

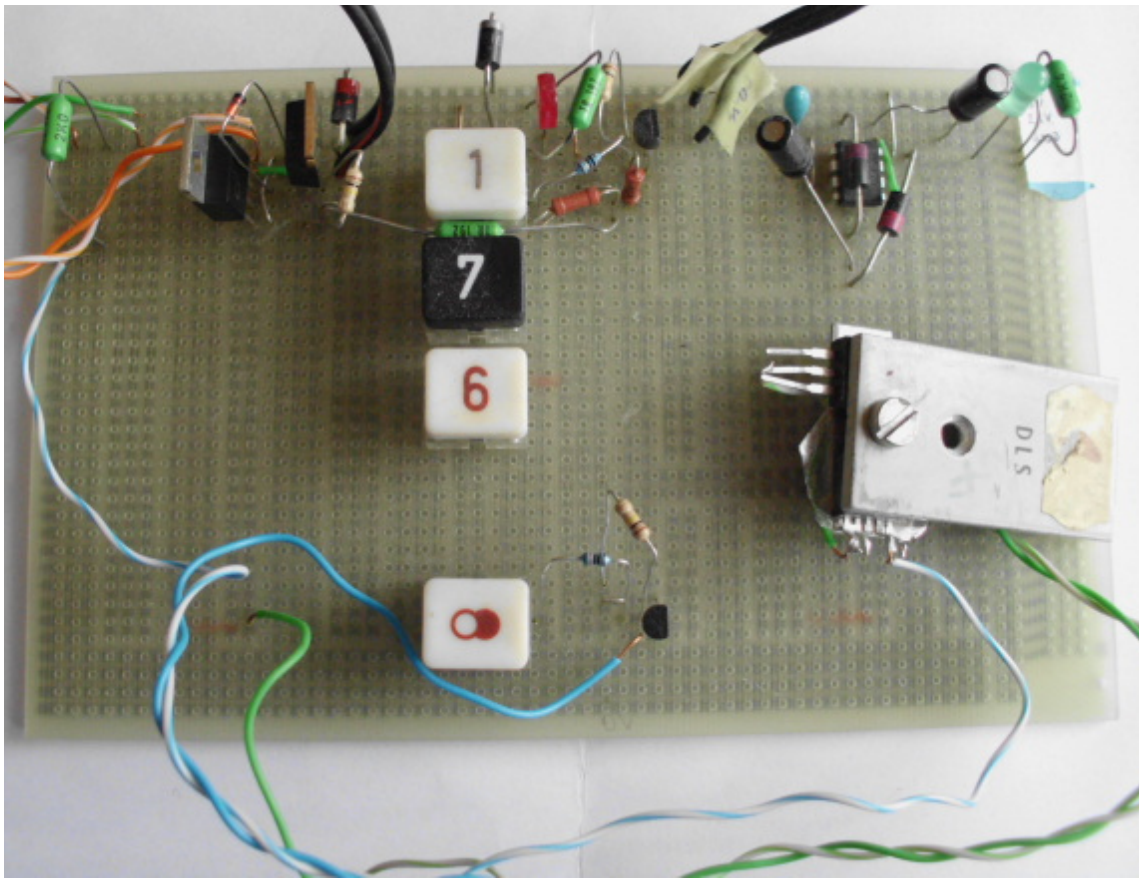

Fig. 2.4: Test implementation of second design of power switch

Third Design

As was already mentioned, the third design is a simplification of the second design. It is based on fact that the path connecting a battery with solar panel and a path connecting a battery with load do not have to be separate and can be combined into one, as was shown in block diagram 1.3.

Its schematic is shown in Fig. 2.5. When compared with the schematic of the previous design in Fig. 2.3, it can be seen that it was created by simply omitting the right half, that was connecting the battery to load. The power line that used to be called TO_S_PANEL has become TO_S_PANEL_&_LOAD. It is clear that the biggest changes have been made on a system level.

This systematic solution seems to have a potential disadvantage, that it is not possible to control whether the connected battery is going to be charged or discharged, as it depends on the instantaneous power fed by solar panel and used by load.

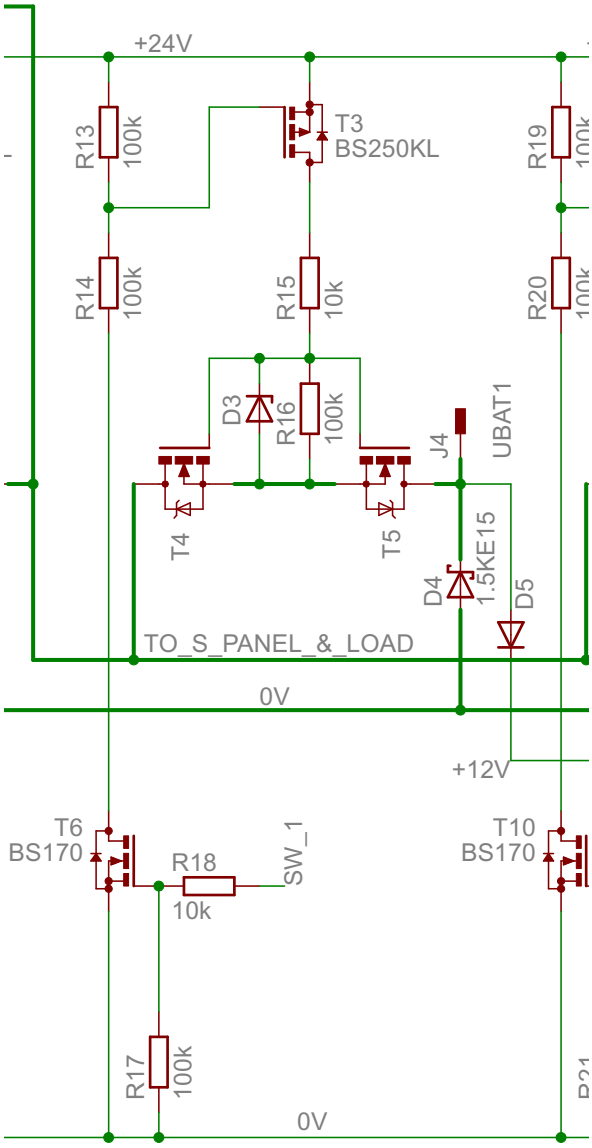

Fig. 2.5: The schematic of a power switch for one battery – third design

Both of these will change independently of each other. But thanks to the measurement of current from solar panel and to load the measured difference in current can be used to determine if we are charging or discharging the battery. So if the control algorithm decides some specific battery needs to be charged and a different one discharged, it can switch between them according to results of current measurement. This shows that this design can be used without the loss of generality for the control algorithm, provided that the currents from solar panel and to load are measured.

On the other hand, this solution has several advantages:

- There are fewer high current paths, which will simplify the design of PCB and make more space so that the paths can be made wider.

- There will be smaller losses than if there were two paths – if there is both current from panel and to load, part of the current will flow directly to load, thus decreasing losses thanks to shorter path.
- Fewer parts are needed – the regulator can be made smaller or it may be possible to control more batteries on the same area of the board.
- Fewer microcontroller pins are needed for more batteries – only one switch for one battery plus two switches for controlling solar panel and load, opposed to two switches per battery.

2.1.2 Current Measurement

The need for the measurement of current from solar panel to batteries and from batteries to load originates in the requirement for power measurements. It should be implemented also if the regulator worked according to the design described by updated block diagram (Fig. 1.3). The current flowing to the load can be used for detecting over-current conditions as well.

Principle and Selection of Implementation Method

Firstly we must define what properties of the current measurement circuit are of the biggest concern. These are:

- precision (the more precise the better),
- range (0-20A nominal),
- low voltage drop on measurement device, and
- price.

As the current to be measured is DC, there is a limited amount of proven solutions available. The following main methods have been considered:

- measuring a voltage drop on a shunt resistor, and
- using specialized measurement ICs.

The first method is simple and may be very precise, but there are several disadvantages in our application. Due to big range of current to be measured the shunt resistor would have to be very small. Even with the shunt resistor with resistance as low as 10mΩ there would be considerable power dissipation on it if highest nominal current flew through it:

$$P_{max} = R \cdot I_{max} = 0.01 \cdot 20^2 = 4W \tag{2.4}$$

This heat dissipation would pose big problems with the change of the resistance of material because of temperature coefficient. Moreover, it would increase the overall consumption of the device.

Another disadvantage is that the voltage drop on such shunt would have to be amplified, which would increase the complexity of the design.

It is also possible to measure the voltage drop on a MOSFET switch or a PCB track (as is described in [10]), but these modifications suffer from the same problems as using the shunt resistor in this design. Moreover the voltage drop on MOSFET is very dependent on temperature.

There are specialized current measurement integrated circuits on the market nowadays. Most of them are in fact Hall effect sensors with integrated signal conditioning circuitry. These are the products that were considered more closely:

- Hall Effect-Based Linear Current Sensor ICs from Allegro microsystems – the ACS75x family [11]. These sensors feature very small resistance (100µΩ) and typically less than 4% total error from -40 °C to 150°C. The devices from this family were considered, but there was a problem with the availability of the part at a time of decision which technology to use.
- Small sized current sensor CQ-121E from company Asahi Kasei Microdevices Corporation (AKEMD) [12]. This part has not been considered either because of the same reason – no retailer for this part has been found.
- Inductive Analog Current Sensors from Honeywell, such as (CSLA2CD or CSNE151). These sensors are available, but they consume considerable amount of power (CSLA2CD – 20mA [13], CSNE151 – 10mA [14]) and are quite costly (about 15 Euros per one piece in Dec. 2010).
- Programmable current sense high side switch IR3313 from International Rectifier. This IC features 7mΩ on resistance, 2% error if calibrated, short circuit protection and thermal protection for the price of about 5 Euros per piece. Its datasheet can be found in [15].

The IR3313 device has been chosen for this application, because the output signal does not need to be amplified (no added complexity), it is available in online stores and the built in short circuit protection feature will further simplify the design of the regulator (it will eliminate the need for separate module to achieve this goal).

Implementation

The basic circuit connection of the IR3313 devices can be seen in Fig. 2.6. The explanation below will concentrate only on one of the circuits shown (namely IC1), as the important characteristics are equivalent also for IC2.

Intelligent switch is controlled by the voltage difference between VCC and IN pin. If T1 is turned on, the voltage difference between the two pins is higher than the specified threshold and IC1 turns on as well. A current proportional to the current through the integrated power MOSFET is sourced to the IFB pin (current

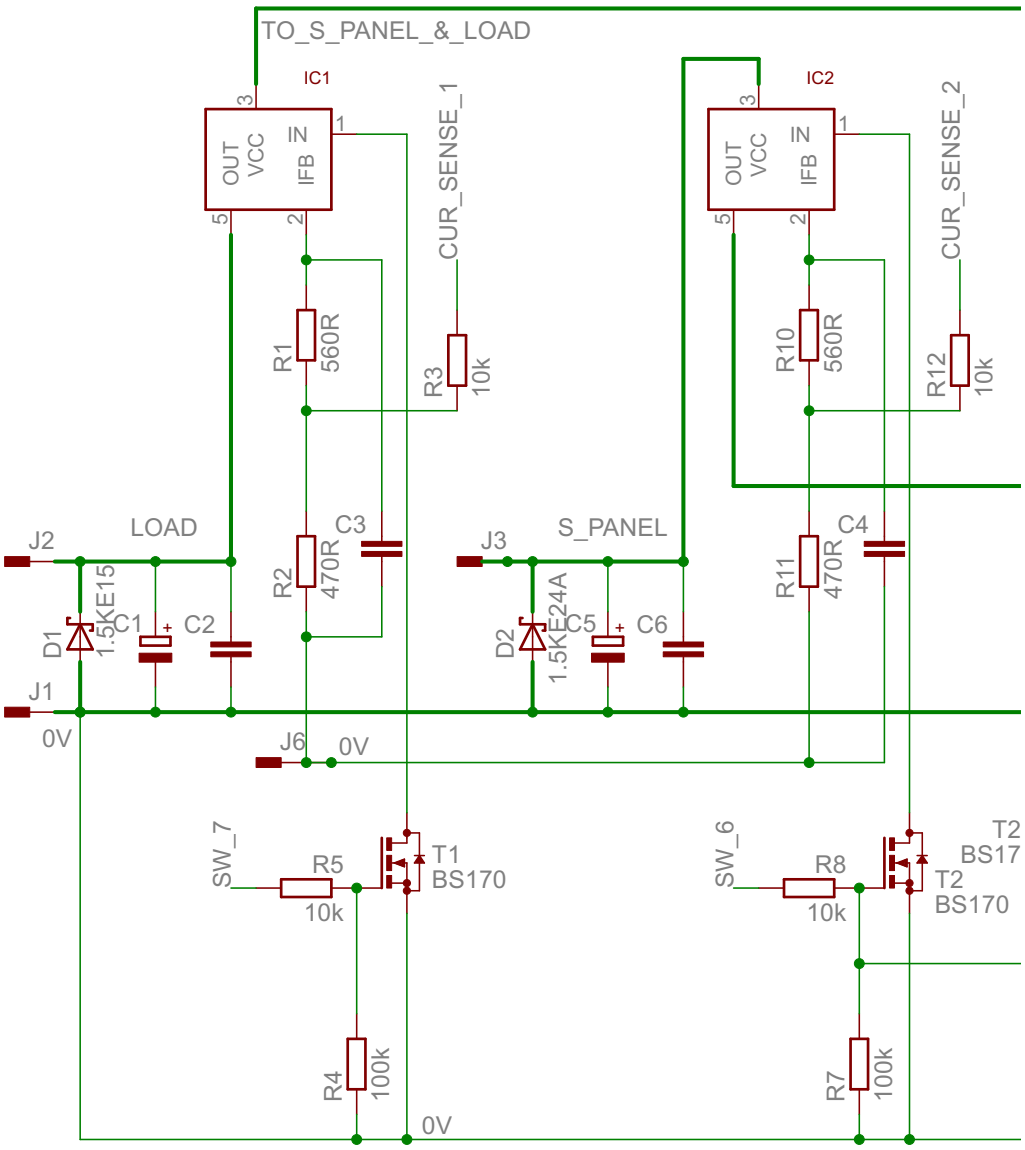

Fig. 2.6: The connection of IR3313 current measurement ICs in the circuit

feedback). If the voltage between IN and IFB pin is higher than about 4.7V, the over current condition is detected and the switch is turned off [15]. The current shutdown threshold is adjusted by selecting the proper resistor between IFB and ground.

The implementation devised for this application uses similar structure as is recommended in the datasheet (the feedback resistor R2, resistor R3 and transistor T1 for turning the IC1 on). The schematic includes also capacitor C3 in case there was excessive noise that would have to be eliminated. This part will be soldered into PCB only if it is needed.

Resistor R1 together with R2 form a voltage divider that can be used to decrease the voltage going to measurement circuit and therefore eliminate the need for divider at the input of ADC.

The values of R1 and R2 are chosen according to several criteria. One of them is to set the over current shutdown threshold to a specific value. This value depends on a sum of resistances of R1 and R2 and should be higher than the nominal voltage, because of the inrush currents when using certain loads (e.g. filament lamps). According to application note for IR3313 [16], the inrush current can be as high as 7 times the nominal current. Therefore the threshold should be higher than the designed nominal current of 20A.

As there is a low chance that there will be filament lamps of high wattages used, we suppose there will be more lamps with lower wattages. By using our judgment we estimate that setting the current threshold to about the double of nominal current should be sufficient. If the practical experience shows later this value is underestimated, the value of R1 and R2 can be changed later if needed.

As was already mentioned, the 4.7V threshold of IR3313 over-current shutdown should represent about 40A, so the desired value of resistors in feedback branch can be calculated:

$$R_1 + R_2 = \frac{V_{threshold}}{\frac{I_{max}}{Ratio}} = \frac{4.7}{\frac{40}{8800}} = 1034\Omega, \tag{2.5}$$

where Ratio is the ratio between the current through the power MOSFET of IR3313 and the current sourced to IFB pin provided by datasheet [15].

Note that setting the over current threshold on IR3313 power switch to value higher than the nominal value for the regulator does not decrease the safety of the device, as the over current conditions lasting longer can be detected by program in microcontroller based on reading from the current measurement circuitry and the load will be disconnected if the condition lasts more than predetermined period of time. But the overcurrent shutdown feature of IR3313 will still be able to protect the device during short circuit conditions.

2.1.3 Voltage Measurement

The measurement of battery voltage is the most important measurement in the charging regulator application, as the operating conditions of lead-acid batteries are determined according to their voltage.

Moreover, in our application the current sensing is achieved by changing the feedback current from IR3313 circuit proportional to the measured current through power MOSFET to voltage on a sense resistor. That is why this measurement is essentially voltage measurement as well.

In the following chapters the required precision of an ADC will be discussed, as well as the supporting circuitry such as voltage reference and protection on ADC inputs.

The need to use an ADC comes from the fact that the charging logic will be implemented using a program running on a microcontroller chip. Its selection will not be described in this chapter, as there is a possibility to use dedicated ADC or one integrated in a microcontroller. This decision process will be mentioned in a section about choosing the microcontroller (2.1.5).

Required Precision

The resolution required for an ADC can be determined according to a maximum error that is acceptable for the measurement. This error can be compared to quantization errors for a several ADC resolutions and the resolutions that produce smaller errors can be chosen. Of course the quantization error is not the only error the ADC produces. There are errors due to Differential nonlinearity, Integral nonlinearity and others as well. These depend on the exact device used, so they will be considered upon selection of an exact device from a set of particular type (such as 10-bit or 12-bit ADCs).

The required precision depends on maximum allowable error of these measurements:

- battery voltage measurement,
- PV voltage measurement, and
- voltage measurement for a current measurement circuitry.

Firstly, the battery voltage measurement is considered. The required precision for a battery voltage monitoring has been found in literature only for the *float voltage* ("constant voltage that is applied continuously to a voltaic cell to maintain the cell in a fully charged condition" [18]). This value is ±0.05V [5]. As this is probably the most critical part of charging cycle, this value is considered as satisfactory for all phases of charging cycle.

The maximum absolute error on the battery terminal has to be recalculated to a maximum quantization error on an ADC's input, because a voltage divider will be used on ADC input:

$$\delta_{\mathrm{BAT}} = \frac{\Delta V}{V} = \frac{0.05\mathrm{V}}{15\mathrm{V}} = 0.00\bar{3} = 0.\bar{3}\%, \tag{2.6}$$

$$\Delta V_{\mathrm{ADC}} = \delta_{\mathrm{BAT}} \cdot \mathrm{ADC\_range} = 0.00\bar{3} \cdot 2.5 = 8.\bar{3}\mathrm{mV} \tag{2.7}$$

One digit in an 8-bit ADC conversion result when using 2.5V voltage reference corresponds to:

$$\Delta V_{\mathrm{bit}} = \frac{2.5}{2^8} = \frac{2.5}{256} \approx 9.77\mathrm{mV} \tag{2.8}$$

The quantization error is equal to half of the smallest unit of resolution, so it is clear that the 8-bit ideal ADC would be satisfactory.

Secondly, the same approach could be used with measurement of voltage on photovoltaic panel input, but it is not necessary as this measurement is only informative. The measurement result will be used only for comparison of voltages on PV panel and battery in order to determine whether the panel is acting as a source of power. At a time of night the panel is not able to produce energy because there is no light to convert and can act as a load for the batteries. The measurement is in place to recognize this situation in order to be able to disconnect the panel from the batteries in such situation.

Thirdly the required precision for current measurement purposes is calculated. According to datasheet of current sensing part IR3313 [15], the error after calibration can be 2%. So the absolute voltage error on an ADC would be:

$$\Delta V_{\mathrm{ADC}} = \delta_{\mathrm{I\_sense}} \cdot \mathrm{ADC\_range} = 0.02 \cdot 2.5 = 50\mathrm{mV} \tag{2.9}$$

It is clear that the circa 10mV quantization error of 8-bit ADC will be much smaller than this error due to current measurement, so again an ideal 8-bit converter would be satisfactory.

In order to be able to really guarantee this required precision, an ADC with higher resolution will have to be used. This higher resolution will have to be high enough so that other errors, such as integral and differential nonlinearities will not affect the minimum 8-bit resolution. As these nonlinearities are usually around one LSB, the 10-bit ADC should be appropriate for this use.

An Application Note (AN) from company Atmel (AVR450, which can be found in [19]) can be used as a simple verification of these minimum precision calculations. This AN shows a reference design of a universal charger for more battery types, including Sealed Lead-Acid batteries. A microcontroller with a 10-bit ADC is used in this application which also shows the conclusions above should be correct.

Voltage Reference

The schematic for this reference can be seen in Fig. 2.7. The IC2 is LM4040-2.5, a precision micropower voltage reference. Its output is 2.5V and it will be used as an input to microcontroller's analog reference (AREF) pin for the A/D converter.

Note that the LM4040-2.5 is only two pin device, but the schematic has been devised so that an adjustable (and hence 3-pin) voltage reference in a TO-92 package can be used. This way the reference voltage or the type of Integrated Circuit (IC) used can be changed later easily, if further optimizations of this design are carried out. The resistors R3 and R4 are to be used only in case an adjustable voltage reference is used.

The value of R5 has been determined according to the recommendations in LM4040-2.5's datasheet for using the LM4040 as shunt regulator [20]. The R5

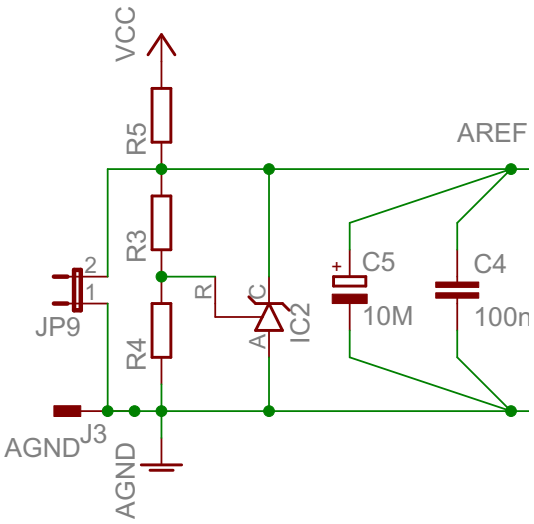

Fig. 2.7: Scheme of voltage reference circuit

should have a value small enough to supply at least minimum acceptable quiescent current (I_Q) to LM4040 when input voltage is at the minimum and load current (I_L) at its maximum. On the other hand, when supply voltage is at its maximum and load current at its minimum, R5 should be large enough to limit the current through LM4040 to 15mA maximum. In case of LM4040-2.5 I_Q is equal to 60µA. The datasheet provides this formula for calculating the series resistance (R_S) (in our scheme R5):

$$R_S = \frac{V_S - V_R}{I_L + I_Q}, \tag{2.10}$$

where V_S is the supply voltage and V_R the LM4040's reverse breakdown voltage.

In order to be able to use this formula, the load current has to be known first. In this case, the ADC of a microcontroller will be the load. The current it may consume can be calculated using the resistance of reference input (R_{REF}) value from the datasheet of an ADC (the substituted values are for an integrated ADC in microcontroller whose selection will be described in Section 2.1.5):

$$I_L = \frac{V_R}{R_{REF}} = \frac{2.5\text{V}}{32\text{k}\Omega} = 78.125\mu\text{A}. \tag{2.11}$$

So by substituting the I_L into Formula 2.10, the R_S can be calculated:

$$R5 = R_S = \frac{V_S - V_R}{I_L + I_Q} = \frac{(5 - 2.5)\text{V}}{(78.125 + 60)\mu\text{A}} \approx 18.1\text{k}\Omega. \tag{2.12}$$

In order to be sure the LM4040 has enough power also in worst conditions, the 16kΩ value was used rather than calculated 18kΩ.

The LM4040 has been chosen as a voltage reference due to its high precision, TO-92 package and the fact it can be used as a shunt reference with no adjustments. According to a distributor its tolerance is ±0.1%, compared to ±1% of other commercially available voltage references.

The capacitors C4 and C5 in Fig. 2.7 are ceramic and tantalum capacitors respectively with values as recommended in LM4040's datasheet [20] for use with ADC. The jumper JP6 is intended to be used as a connector for external voltmeter for calibration of the device and control of correct functionality.

Input Signal Conditioning (Voltage Divider)

The input signals to the ADC have to be processed firstly because most of the measured voltages (on the inputs from batteries and solar panel) are several times higher than the reference voltage. The voltage divider is used for this purpose.

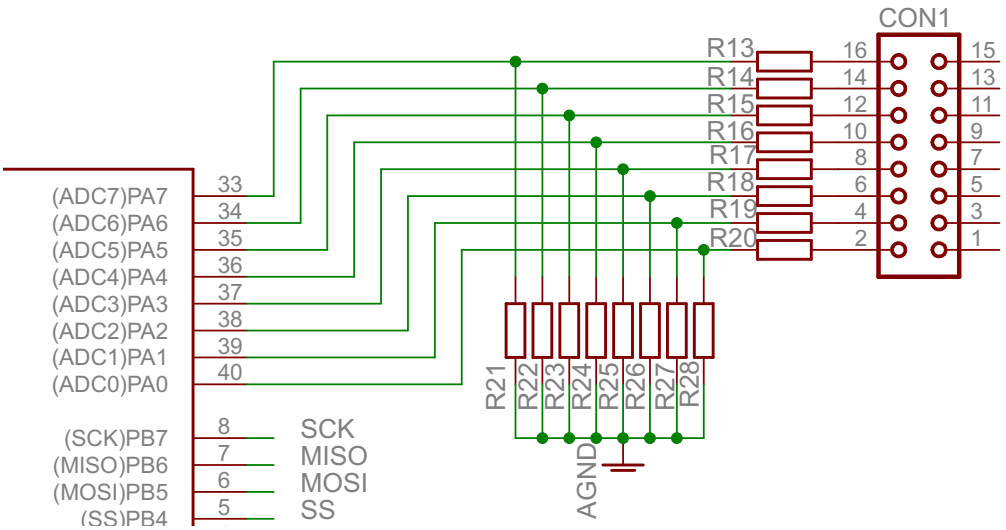

Fig. 2.8: Schematic of input circuitry for ADC

Fig. 2.8 shows the voltage divider consisting of resistors R13 to R28 connected between the measured voltages (connected via connector CON1) and inputs of the ADC.

The resistors R21 and R22 do not have to be used, as there should not be a need for a voltage divider on a current measurement circuit. They are there only in case there was some change later. The R13 and R14 can be used as series resistors for protection of ADC input pins. Ideally their value would be 5kΩ and the value of R3 and R12 in Fig. 2.6 will be changed to 5kΩ as well.

2.1.4 Short Circuit Protection

The built in over current protection of IR3313 power switch will be used as a protection against short circuit condition on the output pins. Its big advantage is that it is fast enough to protect the switch itself and very easy to implement. As the rest of the power transistors are connected in series with IR3313 switch measuring current from the panel or to the load and their maximum current rating is higher than one of the IR3313 switch, they should be protected as well.

The details of the over current protection of IR3313 part and its implementation in this design are covered in Section 2.1.2.

2.1.5 Microcontroller

This will be the most important part of the system, as it will execute the charging algorithms. The selection of this part will be discussed in the first subsection. Then the design of supportive circuits such as reset pin connection and quartz crystal oscillator will follow.

Selection

Below is the description of the main selection criteria.

Package — as there could be a problem with soldering tiny packages without experience or proper tools, the older dual in line (DIL) packages are preferred over the packages for the Surface Mount Device (SMD) technologies.

Number of pins – the higher the pin count, the better, as with higher pin count the regulator can be constructed for more batteries.

Integrated ADC – its presence in a µC will save the need for an external part and thus simplify the final design.

Availability and price – the availability of the device is a must and an adequate price is desirable as well. As the purpose of the final device is to provide economic advantage, it should not be too expensive and thus the main components should have appropriate price as well.

Availability of the programming software and programmer – the µC would be useless without the programmer and appropriate software. It should be available at university or cheap enough to be bought.

Communication interface – the µC should have at least Universal Asynchronous Receiver/Transmitter (UART) as a serial communication interface. This is not an issue nowadays, as most of the microcontrollers do have some sort of or several communication interfaces.

Enough memory – the controller should have enough program memory or at least have a pin compatible part that has more memory so that it can be exchanged later when the exact memory requirements of the software (SW) are known.

Experience with the platform – it is an advantage if the author already has an experience with programming such microprocessors or knows someone who does in order not to spend too much time getting to know the platform. Of course this criterion has a smaller weight than factors that impact functionality.

The products from several manufacturers have been considered. Among these was the MSP430 architecture from Texas Instruments, the products from Freescale, the ATmega family from ATMEL and PIC family from Microchip.

The winning device was the ATmega32A from ATMEL thanks to the fact that it comes in DIL40 package, has a built in 10-bit ADC that is satisfactory for the required precision, has 32kB of flash memory and pin-compatible replacement with twice as much memory (ATmega64). Moreover the ATMEL company offers its development tool AVR Studio for free and USB programmers are available for low enough price. The microcontrollers are available in local stores as well as in specialized internet shops with electronics and the author of this thesis does have a previous experience with this platform.

The rest of the devices were mostly not available in DIL packages with higher pin count or had more expensive programmers or development software. That were their biggest disadvantages that caused they were not selected.

ATmega32A is an improved low power version of ATmega32. They are pin-compatible and the only difference for the designer should be the different reset pull-up resistor value in ATmega32A [21].

Supportive Circuits

Quartz crystal oscillator A standard quartz crystal in HC-49U package has been chosen for this application. The connection is as recommended in datasheet of the µC: Apart from crystal oscillator there are used also two capacitors of nominal value 22pF between the XTAL pins and ground [22].

Reset pin connection The circuit has been devised as recommended in [23]. The schematic can be seen in Fig. 2.9. It includes the pull up resistor R1 that ensures the RST signal is not low when not intended (the reset on ATmega32A is active in the low state). The capacitor C3 is recommended as an additional protection against voltage spikes that could cause unintentional reset.

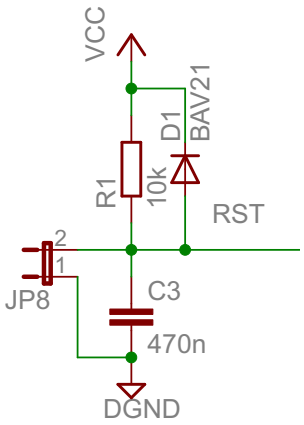

Fig. 2.9: Schematic of a reset circuit connection

In our application the capacitor C3 has a more important function. Together with R1 creates a timing circuit. The time constant determined by their values has been chosen high enough to ensure the µC stays in reset until the power stabilizes. It was estimated that about 5ms should be sufficient time. If not, the values of R1 and C3 can be changed later.

The jumper J8 has been added as a connector for an external pushbutton switch that can be used to reset the µC. Closing the switch will discharge the capacitor C3, bringing the potential on RST to 0V. This resets the microcontroller if the reset pulse is 1.5µs minimum [22]. This is ensured as the time constant for charging C3 via R1 is much higher than this value.

A diode D1 for protection against electrostatic discharge (ESD) is included per instructions in [23] for cases when high voltage programming is not going to be used. The reason is the reset pin does not contain such a diode internally as all other pins, because it is to withstand +12V that are typically applied during high voltage programming.

2.1.6 Voltage Regulator

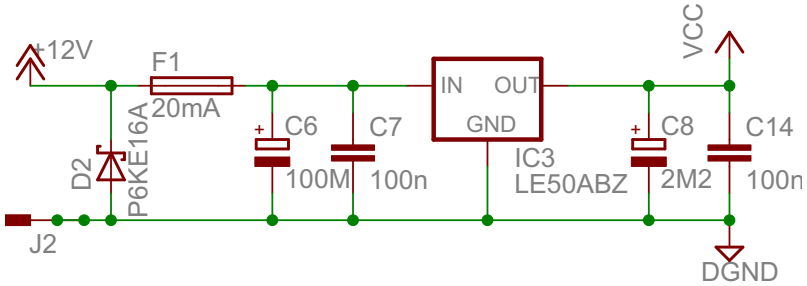

Fig. 2.10: Scheme of the voltage regulator

Since the microcontroller that will be used needs 5V for operation and the available supply gives about +12V, the voltage regulator for powering the µC is necessary. The schematic for the source of +5V can be seen in Fig. 2.10.

As the regulator has been chosen part LE50ABZ thanks to its very low quiescent current. The maximum quiescent current is only 1mA when not loaded and 3mA when supplying maximum current to the load (100mA) according to the datasheet [24]. As the low power consumption of the whole solar regulator is of big importance, this value was the most important selection criterion. It is even lower than the quiescent current consumption of most switching regulators that were considered for power supply of logic as well.

The capacitors with the same values as C7 and C8 in Fig. 2.10 are recommended by the LE50ABZ's datasheet. The capacitor C6 has been added in case this part was not available and a replacement part needed bigger capacitor on input. It can be also used to improve power stability. Ceramic capacitor C14 is included for noise filtering purpose as the C8 of such big value is not common in ceramic technology and electrolytic capacitors have worse performance for higher frequencies.

The Transient Voltage Suppressor (TVS) diode D2 and fuse F1 have been added for protection purposes and their use is discussed in more detail in Section 2.2.3.

2.1.7 Protection Against Reverse Battery Connection

This feature is important as the number of cable connections to the regulator is going to be higher. This increases the chances of making a mistake when connecting the wires. If such a mistake occurred when connecting batteries, the device could be damaged by very high currents the lead-acid batteries are able to supply.

A very simple implementation of this protection has been chosen. It consists of a diode connected to each battery input to the regulator in such a way, that the diode conducts if the battery polarity is reversed. Each battery must be connected via a fuse. This fuse will disconnect the battery from the solar regulator once the battery connections are reversed and the diode on input shorts it to the ground.

In order for this protection to work well the diode has to be able to withstand the high currents which will be limited by the internal resistance of wrongly connected battery and the fuse used. The TVS diodes have been chosen for this purpose. They are able to withstand much higher currents than ordinary diodes and even if they are destroyed by the flowing current, they stay in the conducting state.

Moreover, these diodes are able to protect the device from the dangerous voltage spikes if the battery inputs are accidentally connected to higher voltage, or from a static electricity discharge which could come from e.g. a human body when the inputs are not connected to batteries.

In order to protect the battery inputs from both reverse battery connection and voltage spikes the unidirectional TVS diode has to be used. This diode conducts in one direction and in the reverse direction only after reaching a specified threshold (a lot of values are available).

The voltage rating of TVS diode has to be selected so that the diode does not affect the circuit under normal operation. This means the diode should not conduct until voltage on the batteries is higher than about 14.1V, which should be the maximum voltage to which the lead-acid batteries can be charged. This parameter of TVS diodes is called Stand-off Voltage.

On the other hand, the higher the nominal voltage of the diode the higher is the Clamping Voltage, which is the maximum voltage that can appear on a protected device under the Rated Peak Impulse Current [25]. So to minimize the impact of a surge condition the nominal voltage of the protection diode should be as low as possible (limited by the Stand-off Voltage).

Another factor to consider when choosing the TVS diode is the Peak Pulse Current and the amount of energy the diode is able to absorb. The peak current for protection against reverse battery connection is limited by the fuse used which could be about twice of the nominal current of the solar regulator (hence 40A). This is not a problem for most of the TVS diodes. However, the peak current caused by the possible surge can hardly be calculated. Several methods have been studied in literature, but most of the calculations rely on knowledge of the maximum possible surge current, which is usually guessed depending on the application. So in order to be safe the TVS diode with biggest surge current and energy rating have been selected.

This protection has been included in the schematic for each power switch and can be seen in the center of Fig. 2.3 labelled as D4.

2.1.8 Thermal Protection

The protection of the power switches that should be the only thermally stressed parts will be achieved by the built in over temperature shutdown of IR3313 intelligent switch. This feature shuts down the switch automatically at 165°C [15].

As the rest of the power transistors have very similar $R_{DS(on)}$ value and even better temperature characteristics (they are able to withstand higher junction temperatures, e.g. 175°C for IRF3205 that is intended to be used), they should be protected as well, provided that the heat sinks on all the transistors are the same or better. The reason is that they are connected in series with IR3313 switches that should disconnect the load or power from the PV panel should the high current or higher ambient temperature cause overheating of these parts.

An additional thermal protection could be used for final implementations for lower battery counts by mounting a separate temperature sensor on a common heat sink (if a common heat sink is used for more power transistors). The schematic for using an integrated temperature sensor LM335 can be seen in Fig. 2.11.

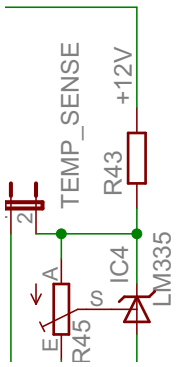

Fig. 2.11: Schematic of temperature sensor for thermal protection

The schematic is based on the schematic of a typical calibrated sensor application in the devices datasheet [26]. The value of resistor R43 will be chosen so that more than the minimum supply current is fed to the device. The 10kΩ trimmer R45 does not need to be used if the calibration is not needed.

The TEMP_SENSE signal will be fed to a spare ADC input. The measured data will enable software shutdown when dangerous temperatures are reached. The temperature sensor can alternatively be used to monitor ambient temperature if the experience from the testing shows the additional protection is not necessary at all.

2.1.9 Keyboard and LEDs

There are three keys intended to be used for the menu and ideally two LEDs to indicate the status of the device (green Light-Emitting Diode (LED) for normal operation and red for error). In order to create a more universal design in which the LEDs and switches could be interchanged or in which the port pins would be used for different function (under some configurations where the LEDs and keys are not necessary) the schematic connection shown in Fig. 2.12 is used.

This could be done thanks to the fact the LEDs and switches are to be mounted on the front panel of the box for the device and connected to PCB using cables connected to some of the jumper pins JP1 to JP7. The switches will be connected between the resistors and ground and the LEDs between the resistors and VCC pins.

Four of the pins will be shared with the SPI interface that will be used for In System Programming that is used for programming AVR devices (ATmega32 belongs to this group). These can be used for the switches, as the programming will

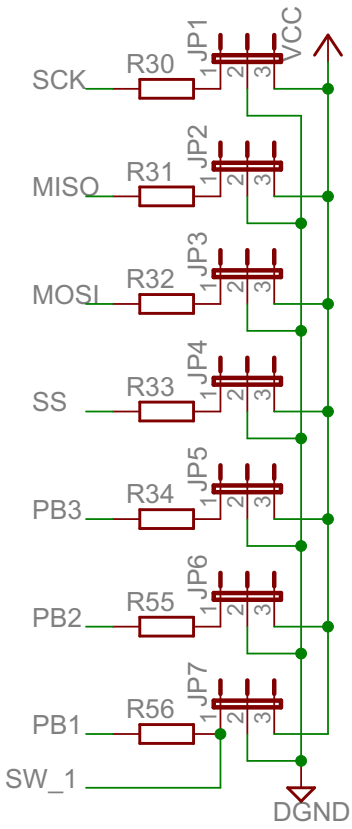

Fig. 2.12: The connections for LEDs and switches for keyboard

be used only in the development phase. But the switches cannot be pressed while the programming takes place.

The LEDs have to be connected to PB2 and PB3 port pins. Some of these port pins can be left unused, depending on the final configuration of the solar regulator.

2.1.10 LCD and LCD Backlight Control

As the majority of alphanumeric monochromatic matrix LCDs are controlled by HD44780 controller or equivalent, the connections to the LCD do not depend on the exact LCD type. So an LCD with 1x16 characters or 2x16 characters can be used without making any modifications to hardware connections.

The schematic in Fig. 2.13 shows how the LCD port pins will be connected to µC pins. The series resistors are added for protection purposes and to be able to use the port pins alternatively, if the LCD is not used. When connected to LCD the resistors R42 to R48 should have low value (about 100Ω). These lines will be used in the following way:

- Four lines for data bus lines (a 4 wire and 8 wire mode are possible and 4 wire interconnection was chosen in order to save much needed µC pins),

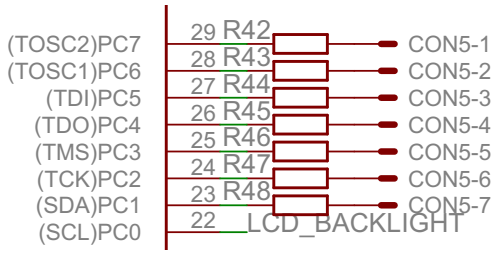

Fig. 2.13: The schematic diagram of LCD connection to PCB and microcontroller

- one line for Register Select, Read/Write and Enable signal each.

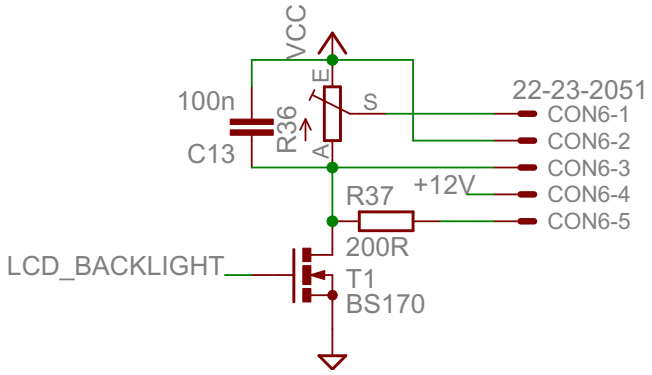

Fig. 2.14: The circuit design for powering the LCD and its backlight

Fig. 2.14 shows the schematic of power supply to the LCD. The first pin of CON6 will supply the adjustable voltage for adjusting the contrast of the display. The potentiometer R36 should have a value between 10 and 20kΩ according to datasheet of the LCD bought for development purposes [27]. The other pins will supply +5V for the logic, GND, +12V for the backlight and the last pin will connect the backlight cathode to ground via a series resistor that will limit the current through the backlight LEDs. The exact value of the R37 should be determined by the measurements of the backlight's current consumption, as the datasheet of LCD used does not specify this value.

Whether the backlight and power supply to LCD is on or off will be controlled by pin PC0 (see Fig. 2.13) that will drive control whether MOSFET transistor T1 in Fig. 2.14 conducts or not. The backlight control has been designed in this way in order not to damage the port pin should the power requirements of the LCD backlight be too high. Note that the backlight is powered from +12V and not +5V. This is done in order not to put too much load on the +5V stabilizer for µC and other logic devices. This has no impact on the efficiency of the regulator, as the voltage difference between the +12V and about 4.2V for backlight operation would be dissipated on the +5V stabilizer in the same way as on the R37.

2.1.11 Battery Temperature Measurement

As there will be more batteries used that can be physically stored apart from each other there may be a need for multiple temperature sensors for the batteries. To prepare for this possibility a temperature sensor DS18B20 from Dallas Semiconductor with digital output was chosen.

Its advantage over temperature sensors with an analog output is that just a normal Input/Output (I/O) pin instead of ADC input can be used and that there can be more of these sensors on a single bus line. It has satisfactory resolution (0.5°C over temperature range from -10°C to +85°C and 2°C over temperature range from -55°C to +125°C [28]) and price comparable to other digital temperature sensors. Moreover, it is quite known and available in many stores and comes in TO-92 package and not only surface mount technology.

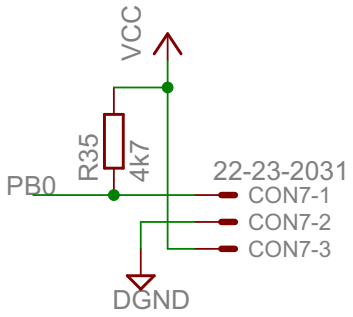

Fig. 2.15: A schematic diagram of connection for DS18B20 temperature sensor

The temperature sensor will be connected as shown in Fig. 2.15. This connection follows the recommendations for powering the DS18B20 with an external supply in the devices datasheet [28]. The R35 is a pull up resistor for the 1-wire bus with nominal value per datasheets recommendation. The leads from CON7 on the PCB board can be ended on a connector mounted on the regulator's box in order to enable easy interconnection of the temperature sensor and mitigating the risk the user connects the CON7's pins in a wrong way.

A second DS18B20 sensor could be used to replace the analog sensor for thermal protection purposes (discussed in Section 2.1.8) if saving an ADC input pin was necessary.

2.1.12 Watchdog

The first intention was to use the external watchdog to reset the device in case the program execution in the microcontroller got stalled. The advantage of an external device over internal watchdog (that is now present in majority of microcontrollers)

is that the internal watchdog can be impacted by the same disturbances (noise, transients) that could cause the main program in the µC to malfunction.

It was considered to use a DS1232LPN+ watchdog from Dallas Semiconductor, because it offers the required functionality (watchdog, power supply monitoring and input for pushbutton reset), low power consumption, is available in DIP technology and has plenty of pin compatible replacements in case this exact part is not available in stores.

However, the added cost and complexity of design due to use of external watchdog and the requirement to dedicate one I/O pin to refreshing the watchdog was finally a stronger argument, so in the final design just an internal watchdog is considered. The reason is also that the rest of the system has been designed to prevent dangerous conditions (short-circuit and overheating of power switches) without the microcontrollers intervention. Therefore it is not critical to ensure the program in µC is executed all the time and the internal watchdog should be sufficient.

2.1.13 Real-Time Clock

An external Real-Time Clock connected through some interface such as Serial Peripheral Interface (SPI) or Inter-Integrated Circuit, also called "two-wire interface" (I^2C) was considered first to be used. After selecting a microcontroller for this application it became clear the external part is not needed at all, since the ATmega32's Timer/Counter2 can be configured as a Real Time Counter. The only thing it needs is the 32.768kHz crystal.

In the final design however there is no need for exact timekeeping, as the data logging will not be done on the µC controlling the battery charging. Another microcontroller may be connected to the regulator via serial communication interface for this purpose. In order not to make the main controller too complicated, the real time clock will be implemented in the µC for datalogging.

2.1.14 Serial Communication Interface

The schematic of circuit for serial communication interface can be seen in Fig. 2.16. The reason why this exact type of transceiver (MAX488) and this type of network (RS485) has been used will be explained in the Section 2.2.1.

The most important part in Fig. 2.16 is the MAX488 RS-485/RS-422 transceiver. This is a low power full duplex transceiver without the receiver and driver enable functionality. The C1 is a bypass capacitor placed close to the MAX488's VCC pin.

Transmit and receive signals from the µC's UART are fed to the transceiver through low pass filters made up from R6, C10 and R7, C9. These are included in

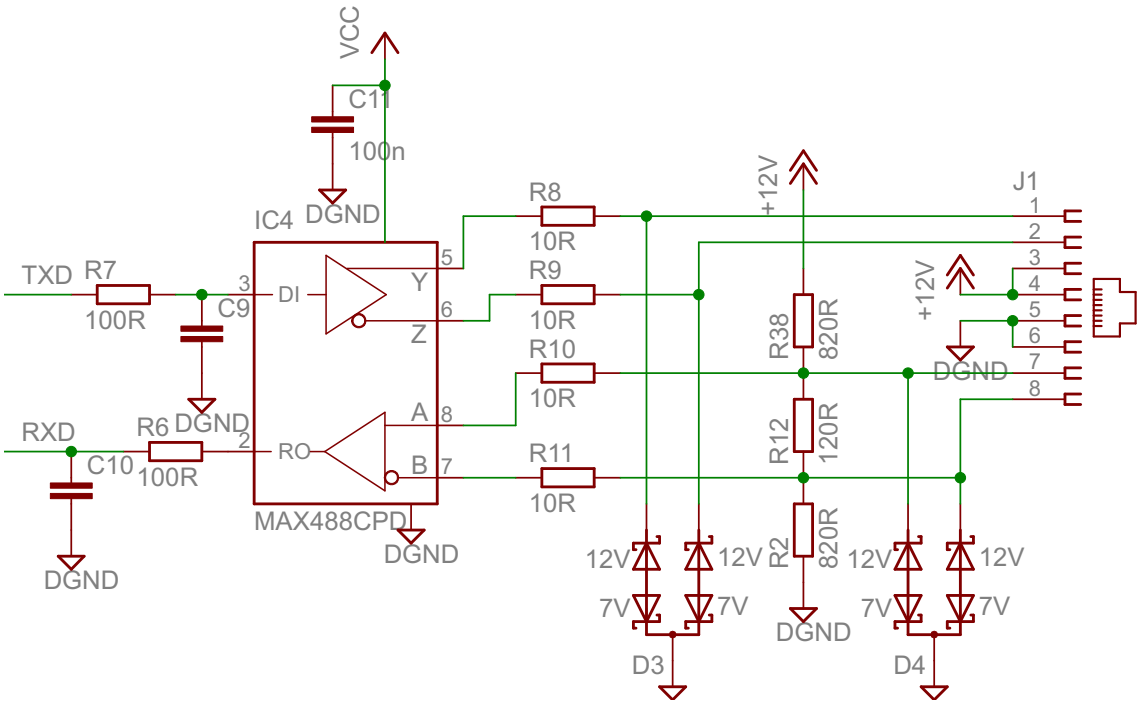

Fig. 2.16: Scheme of the connection of UART to RS-422/485 transceiver

the schematic and board design in case there is excessive noise coming from the transceiver, per several Application Reports from Texas Instruments (such as [29]).

The D3 and D4 are Transient Voltage Suppressor diodes SM712 from Semtech company designed specially for RS-485 application. They are asymmetrical (12V to −7V) which is ideal for the electrical characteristics of RS-485 interface. The resistors R8-R11 are included to further reduce the voltage pulse on the transceiver when the transient pulse occurs on the data bus. These safety measures against electrostatic discharges were applied per recommendations by several manufacturers in their application notes ([30], [29], [31]).

The R12 is the terminating resistor on the receiver end of the line. The transceivers datasheet shows 120Ω terminating resistors [32], but determining the proper value of resistor for an application can be a more complicated task. In case of problems with this interface the value of this terminating resistor may have to be reconsidered.

This scheme contains also fail safe biasing resistors R2 and R38 with the values chosen according to recommendations in [33]. Their purpose is to keep the receiver line in a defined state even if there are no transceivers connected to the bus. In this way the danger of noise causing a false reception is minimized.

The J1 is a RJ-45 type connector that will be used to interface with other

connected devices using Unshielded Twisted Pair (UTP) or Shielded Twisted Pair (STP) cable. The wiring diagrams will have to be created so that the individual pairs are connected so that the noise immunity is as high as possible (the pairs will have to be connected to pins: 1 and 2, 3 and 5, 4 and 6, 7 and 8). The reason is that the twisted pair has only sense if the current through the two wires in the pair is of the same value and opposite direction.

2.2 Incorporating Blocks into System

So far only the individual building blocks have been described. However, the way they are interconnected and also some other considerations such as dimensions of box for the regulator, the size of PCB and other features have to be discussed.

2.2.1 Decomposition of the Control System

Implementing all the required functionality into one controller is possible, but it would increase the complexity of the logic part of the system beyond a practical level. This is true especially for the data logging capability, as it requires accurate timekeeping, large data storage, more complicated program for safe data storage and data transfer to PC.

In order to simplify the design of the microcontroller responsible for charging the batteries, a second microcontroller can be used. Its task will be to take care of the data logging. These two µCs have to be connected by some sort of interface. Out of all the possibilities the RS-485 has been chosen as the best solution, since it is proven in industrial environment, allows a multipoint network topology and is not very difficult to interface with µC.

Another practical step is to decompose the regulator into main part that would be physically located near the controlled batteries and the human interface part which could be placed closer to where the users will spend most of their time. The reason is that as the regulator is built for more batteries and it is expected that these will not be stored in main living area. The reason is the space requirements are supposed to be big and cabling is not very aesthetic. A remotely located unit for interaction with humans – Human Interface Unit (HIU) will therefore have keys for controlling the operation of the regulator and LCD for displaying performance data and status of the system.

The fact the RS-485 network supports a multipoint topology allows all the functions to be divided into 3 units (main controller, HIU and data logger). However, the HIU and data logger units can be combined.

Planned network architecture is shown in Fig. 2.17. As can be seen, a full duplex operation will be possible. As the main controller will act as a master, its transceiver does not really need a Receiver/Driver enable pin. Thanks to this fact the MAX488 transceiver has been selected for the main unit. Its usage is described in more detail in Section 2.1.14.

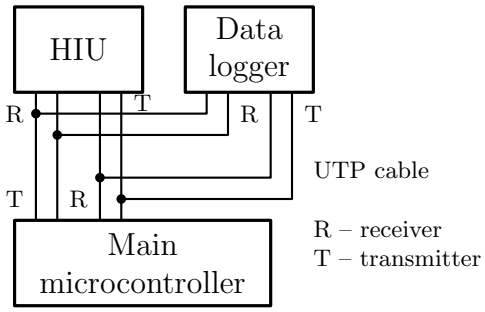

Fig. 2.17: The block diagram of connecting subsystems using RS-485 network

The devices can be connected using an UTP cable out of which two pairs will be used as data pairs (shown in Fig. 2.17) and the other two for powering the remote units (not shown). The main microcontroller will send data to be shown on HIU and measurements to be logged by data logger. The HIU will send the sequence of keys pressed by the user back to the main unit. Data logger does not necessarily need a line for transmitting data to main µC, but is included in case there is a need in the future. This could be for example information from the real time clock in the data logger.

2.2.2 Hardware Decomposition

As the number of parts in the design is quite high, the realization of schematic on one PCB would be quite complicated. Moreover, there are two categories of paths needed. The paths for logical signals will lead just milliamperes of current whereas the paths for the power switches have to withstand high nominal currents of 20A. As a result a logical thing to do is to divide the whole project of PCB into two boards – *logic board* and *power board*.

The power board will contain the switches for each battery, IR3313 intelligent switches, and input protection. The logic board will contain the µC, the RS-485 transceiver and the supportive circuits such as voltage stabilizer, voltage reference and connectors to LCD.

The two boards will be interconnected by two cables. One is dedicated for measured signals (battery voltages, current measurement, etc.) and consists of several signal lines separated with grounded lines in order to minimize interference between

the individual measured channels. The grounded lines will be connected to ground on the power board.

The second cable will consist of lines with logical signals for power switches for the batteries. Two of the lines will be used for transferring +12V and +24V to the logic board in order to power the logic. The +24V is not intended to be used in current design, but it will be interfaced in case it is useful sometimes in future.

The fact that the logical signals for power switches originate on different PCB requires the use of gate protection for MOSFET transistors. The reason is that "all MOSFET devices are extremely susceptible to gate oxide breakdown, caused by electrostatic discharge" [1]. That is why authors of the cited book recommend 1k-10k series resistors for this case. In the scheme of power board it is the resistors R5, R8, R18, etc.

The ground signal (or more precisely the 0V or the common negative poles of the batteries) will be distributed to each board through individual cables of bigger diameter and connected to the board using Faston connectors. There will be several of these wires – one for the ADC ground, one for digital circuits, one for the two IR3313 parts and one for the logic driving the power switches and the TVS diodes used for reverse battery protection.

Also the rest of the high current paths for the batteries can be connected using Faston blade connectors that should be able to withstand such high nominal currents. Alternatively the wires can be soldered directly into the board as is usually done in power supplies in personal computer (PC) that supply high nominal currents as well. In this case the wires can be first directed through a hole of appropriate diameter that would ensure the soldered connection is not mechanically stressed and thus prevent the wire from breaking off the board.

The schematic diagrams for both boards can be seen in Appendix B and Appendix C. Some parts of the final schemes for the boards have not been discussed in the design of the elementary building blocks (Section 2.1) and they will be described in the following chapter.

2.2.3 Additional Concerns/Features

The schematic diagram in Appendix B shows the circuits included in the Power Board. Apart from the current measurement blocks, the power switches and the connectors to logic board, some features have not been described:

Input protection consists of TVS diodes similar to ones used for the Reverse battery protection (Section 2.1.7). They should protect against over-voltage on these connectors and/or from unexpected power source being connected to load connector. The C1, C2, C5 and C6 are included in the design order in

case it will be needed to prevent noise from entering the system. They can be soldered into the PCB in case this problem is experienced (it could happen if some converter from 12V DC to 230V AC was used in the solar system, as these switching converters can produce considerable amount of noise).

Voltage doubler (in scheme labelled as IC3) is used to create the +24V out of +12V available from batteries. This higher voltage is needed by the power switch control circuitry described in Section 2.1.1. There are several pin compatible circuits from different manufacturers that have been selected for this application, such as IC7662 from Maxim or TC962 from Microchip company. These circuits are basically charge pumps, they are very efficient, are able to supply 20mA or more to its load and come in 8-pin DIL package.

Fuses F1 to F3 are used in order to disconnect the power supply for logic in case high currents are drawn (F1, F2 are resettable fuses) or in case the heat sink of power transistors is overheated (F3 is a fuse disconnecting the circuit in case the temperature reaches about 131°C). This is a safety feature, because once the logic board is not powered, no signals for turning the power transistors on can be generated and the regulator should stay in the safe state when no current flows anywhere.

Additional switch (consisting of power MOSFET T24 and associated parts) in series with IR3313 for solar panel (IC2) has been used to make the switch for solar panel bidirectional as well. This way it is possible to prevent not only overcharging the batteries, but also discharging the batteries during the night when the solar panel acts as a load.

There are several things not described earlier in the schematic of Logic Board as well:

Filter for AVCC – AVCC is the power supply pin for the ADC and this pin is connected to +5V via a filter consisting of a capacitor C12 and inductor L1. This topology and the values have been used according to recommendations in the microcontroller's datasheet [22].

Programming connector – there are standard programming connectors for ATMEL AVR devices and a 10-pin connector for SPI programming interface has been chosen and wired according to [23] in the design of Logic Board.

Protecting resistor for µC's pins – these resistors (such as R42–R48 or R49–R54) serve as protection of microcontroller's outputs from accidental connection to ground. Their value has been chosen to be 150Ω, so that if the I/O pin is shorted to ground, the current will be smaller than the absolute maximum of 40mA per pin according to datasheet [22].

2.2.4 Case for HW

As a case for the charge controller was initially chosen case called KT 250. It is universal case for electrical installations and its advantage is that it has been in production for a long time and it is expected that it will be available for a long time as well. It is quite big, so it should have been big enough for the implementation of regulator. Moreover, its price is adequate to the quality of product. Its dimensions and places where screws can be easily mounted (for holding the PCBs) can be seen on a sketch in Fig. 2.18.

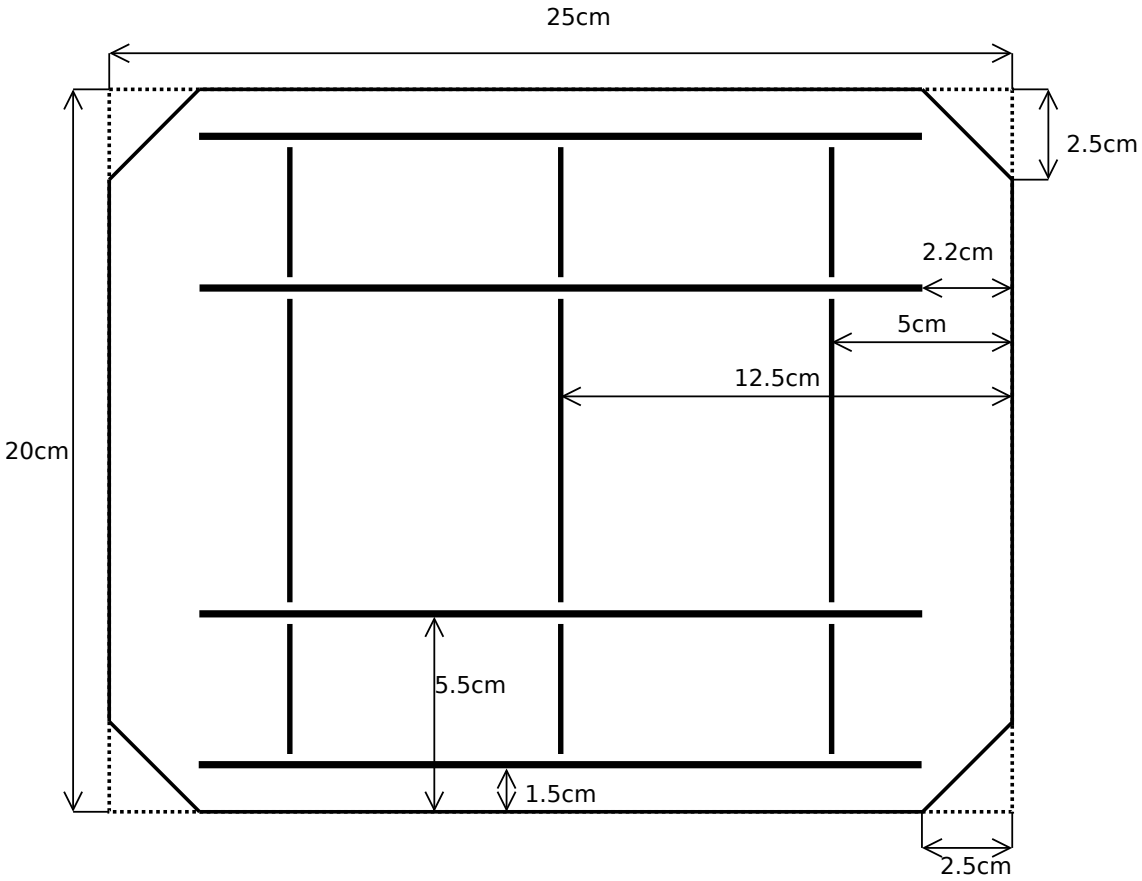

Fig. 2.18: Sketch of dimensions of case KT 250.

The PCBs were designed so that they fit in this case and so that they can be mounted in this case.

Later there was found also a more universal alternative (different case) into which the prototype implementation of the solar regulator has been encased.

2.2.5 Heat Sinks for Power Components

There are only two power components for which it is necessary to determine if and what type of heat sink will be required. These components are power switches,

namely intelligent switch IR3313 and power MOSFET IRF3205.

The need for applying a heat sink can be evaluated using several parameters, such as junction-to-ambient thermal resistance (Θ_{JA}), junction-to-case thermal resistance (Θ_{JC}), case-to-heat sink thermal resistance (Θ_{CS}), case-to-ambient thermal resistance (Θ_{CA}), heat sink-to-ambient thermal resistance (Θ_{SA}), maximum allowable junction temperature junction temperature (T_J), maximum expected ambient temperature (T_A) and the heat dissipation of the component. Most of these parameters can be found in devices' data sheets [15], [17]. The rest has been chosen as is described below.

Firstly the maximum nominal heat dissipation of critical parts has been calculated based on maximum nominal current and the $R_{DS(on)}$ value for each part:

$$P_{IR3313} = R_{DS(on)} \cdot I^2 = 0.007 \cdot 20^2 = 2.8W \tag{2.13}$$

$$P_{IRF3205} = R_{DS(on)} \cdot I^2 = 0.008 \cdot 20^2 = 3.2W \tag{2.14}$$

Then by setting the maximum T_J to be 20°C smaller then absolute maximum for each part (which is 130°C for IR3313 and 155°C for IR3313) and maximum ambient temperature to be 40°C, the need for heat sink was determined. The calculations were done using an online tool for this purpose [35] and verified according to formulas in [34], e.g. for a situation with heat sink:

$$\Theta_{JAtotal} = \Theta_{JC} + \Theta_{CS} + \Theta_{SA} = \frac{T_J - T_A}{P}. \tag{2.15}$$

Calculations showed a heat sink has to be used, with maximum thermal resistance of

$$\Theta_{SA} = \frac{T_J - T_A}{P} - \Theta_{JC} - \Theta_{CS} = \frac{130 - 40}{2.8} - 0.7 - 0.5 = \lfloor 30.94 \rfloor = 30°C/W \tag{2.16}$$

for IR3313 and

$$\Theta_{SA} = \frac{T_J - T_A}{P} - \Theta_{JC} - \Theta_{CS} = \frac{155 - 40}{3.2} - 0.75 - 0.5 = \lfloor 34.69 \rfloor = 34°C/W \tag{2.17}$$

for IRF3205.

A heat sink DO3A for TO-220 cases with perfectly acceptable $\Theta_{SA} = 25°C/W$ has been found. But just to be on the safe side, a heat sink of the same type but with bigger area (DO2A) and $\Theta_{SA} = 22°C/W$ has been chosen and the implementation is made ready even for the biggest DO1A with $\Theta_{SA} = 21°C/W$.

2.3 PCB Design

As the author had no significant experience with the design of PCB and did not want to risk the delay and need to do rework on PCBs should a small detail be omitted

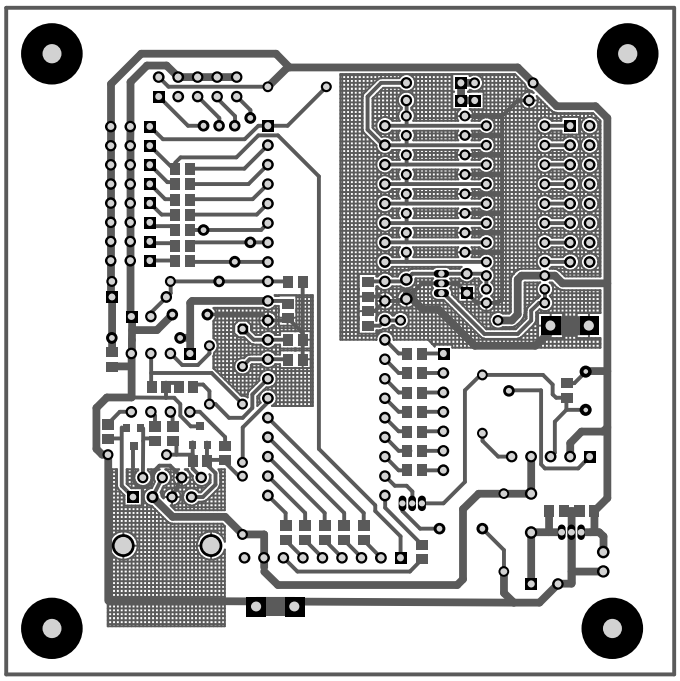

Fig. 2.19: The PCB design of Logic Board

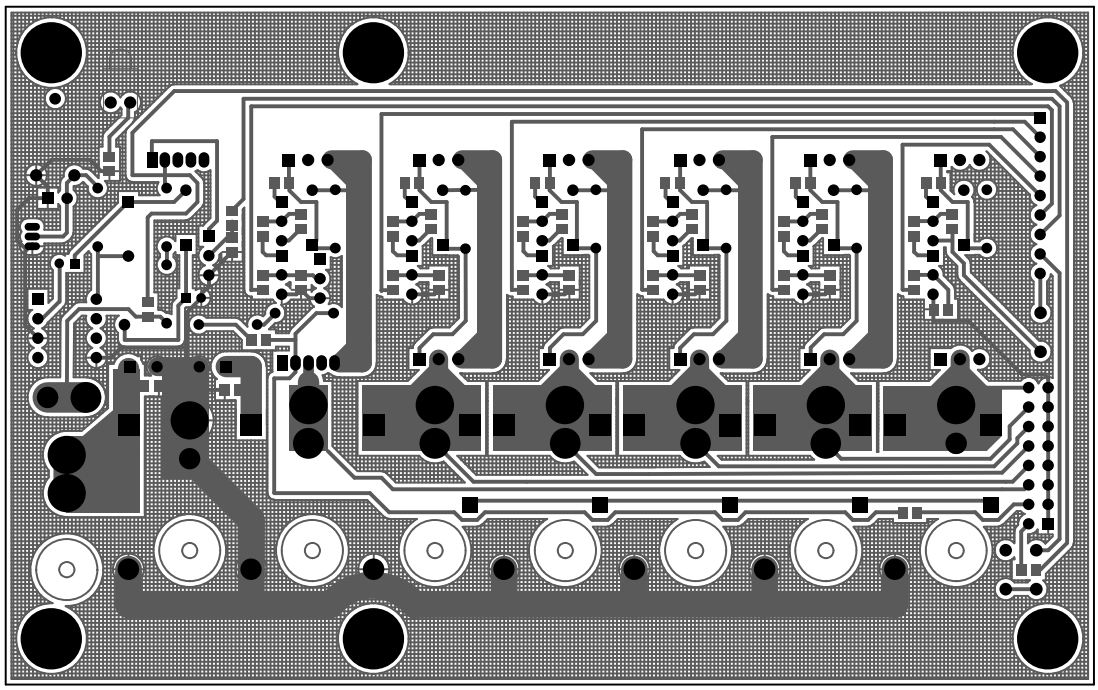

Fig. 2.20: The PCB design of Power Board – bottom

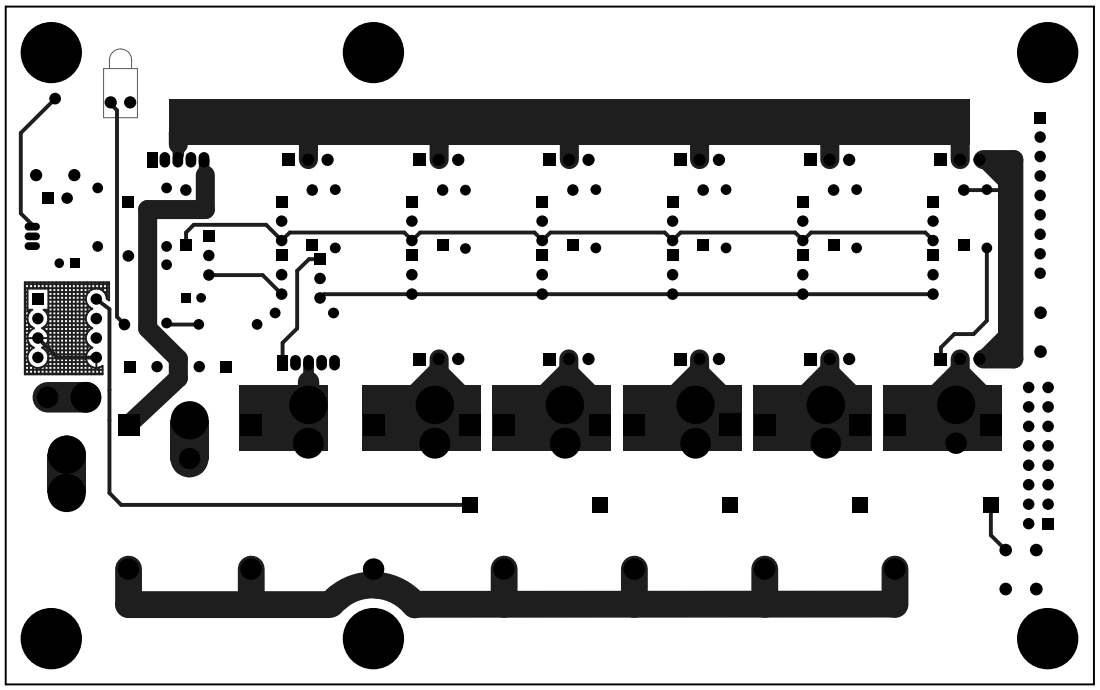

Fig. 2.21: The PCB design of Power Board – top

because of lack of experience, the design of the PCB was left upon the producer of the circuit boards.

The results of several iterations of debugging and improving the design can be seen in Fig. 2.19 for Logic Board and in figures 2.20 and 2.21 for Power Board (this circuit board is two sided).

The Power board was designed so that both ways of connecting the power cables described in Section 2.2.2 (Faston connectors and direct soldering of cable to PCB) could be used. That is why there are a few holes with bigger diameter visible in the Fig. 2.20. If the cables were to be soldered directly, additional holes would have to be drilled in place of Faston connectors where the cables would be actually connected. There are also other issues worth mention regarding the produced design and these will be described below.

2.3.1 Packages of Parts

A lot of electronic parts come in various packages nowadays. Usually they come in some sort of older bigger package (e.g. TO-92, DO-35) that require holes in the PCB for the leads or they are produced as SMDs.

In order to save space on the board, most of the passive components were chosen in SMD packages where possible (the packages 0805 were used).

2.3.2 Trace Width

With the nominal currents planned to be as high as 20A it is neccessary to consider proper path width or thicker conducting material on the PCB, so that the increased heat dissipation does not lead to damage of the board due to thermal stress.

The required width of track depends on maximum temperature of the track to be allowed and the PCB can handle, ambient temperature, the current through the track and the thickness of the conducting material (usually copper) of PCB.

Most common thickness of copper on the PCBs on the market is 35µm. PCBs with thicker conducting material (70µm, 105µm [36]) are sold as well, but there is a problem with their availability. That is why the widely available PCBs with 35µm thick copper layer have been used.

The required trace width for such board, nominal current of 20A and temperature rise of 50°C in air is 7.05mm according to calculations performed using online tool for this purpose [37].

Because it was not always possible to keep the traces this wide (some of them are only 3mm wide) and in order to further decrease the resistance of traces that are within these limits, the traces for high currents have to be covered with a tin solder of substantial thickness (about 1mm or more). This precaution makes the path for currents several times thicker, which should prevent any problems. The application of this technique on prototype of Power Board can be seen in Fig. 2.22.

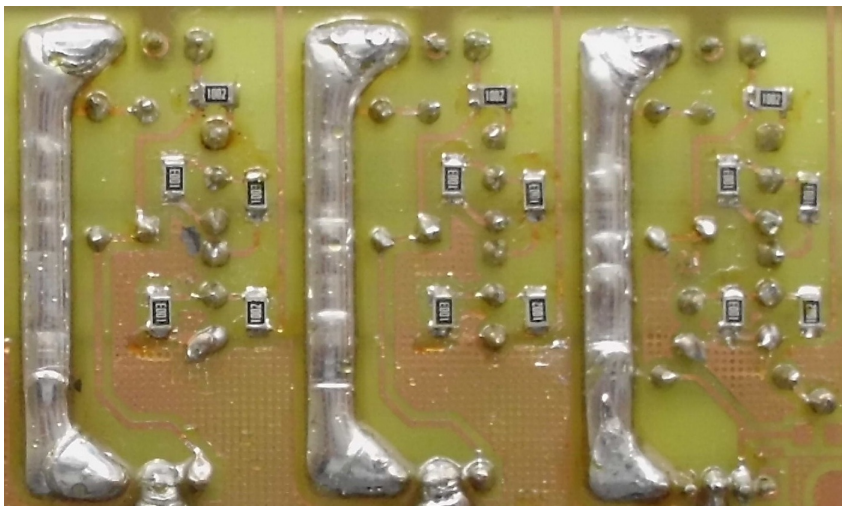

Fig. 2.22: Treatment of high current traces on Power Board

2.4 Prototype Implementation

The prototype realization of the PCB contains all the designed features, except for the temperature sensor on the Power Board and the transceiver for the RS-485 network on the Logic Board. The reason is that these features would be unused at this stage of development.

The picture of prototype implementation of solar regulator (without the case cover) can be seen in Fig. 2.23. The two pairs of wires in the top part of the picture are there only temporarily. They connect the UART with RS-232 transceiver that is connected to PC. This connection was used for debugging purposes during software development, whose results will be described in the next chapter.

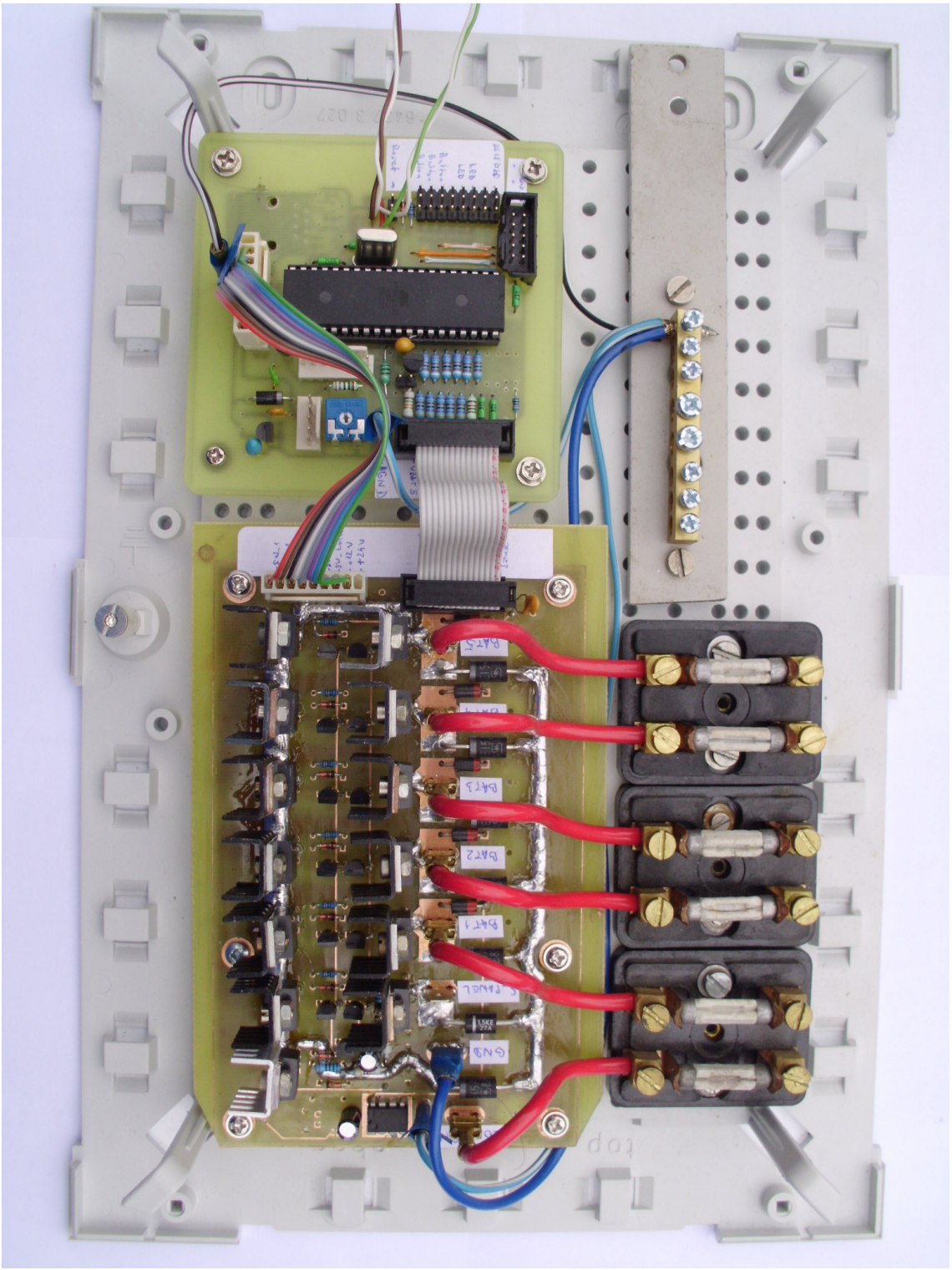

Fig. 2.23: Prototype implementation of the charge controller

3 SOFTWARE DESIGN

The principle design of software for the regulator to be implemented on ATmega32A microcontroller is described in this chapter.

Before going into details, the purpose of the software implementation has to be stated. It is to implement the basic functionality of the controller. It should be simple and work reliably. If this purpose is fulfilled, such implementation can then serve as a baseline for future improvements.

3.1 Main Loop

The main function should execute the functionality shown in flowchart in Fig. 3.1 in an infinite loop. In current implementation the commands in the loop are executed approximately every second.

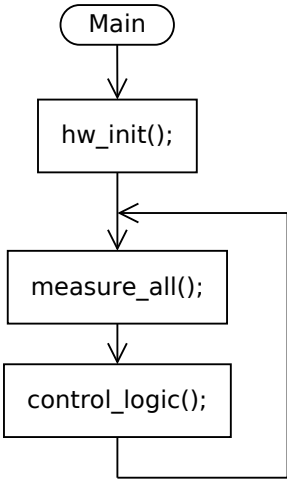

Fig. 3.1: The principle flowchart of main function

The function *hw_ init()* is called only once each time the µC is powered up or reset. It contains commands that set the registry values responsible for hardware functionality, such as direction of I/O ports etc. Other two functions periodically executed by the main function will be described in the following sections.

3.2 Measuring Data

The function *measure_ all()* is responsible for data acquisition on all input channels of the ADC. Its flowchart is shown in Fig. 3.2. Depending on the type of measured signal the charging from solar panel may be temporarily stopped and resumed after

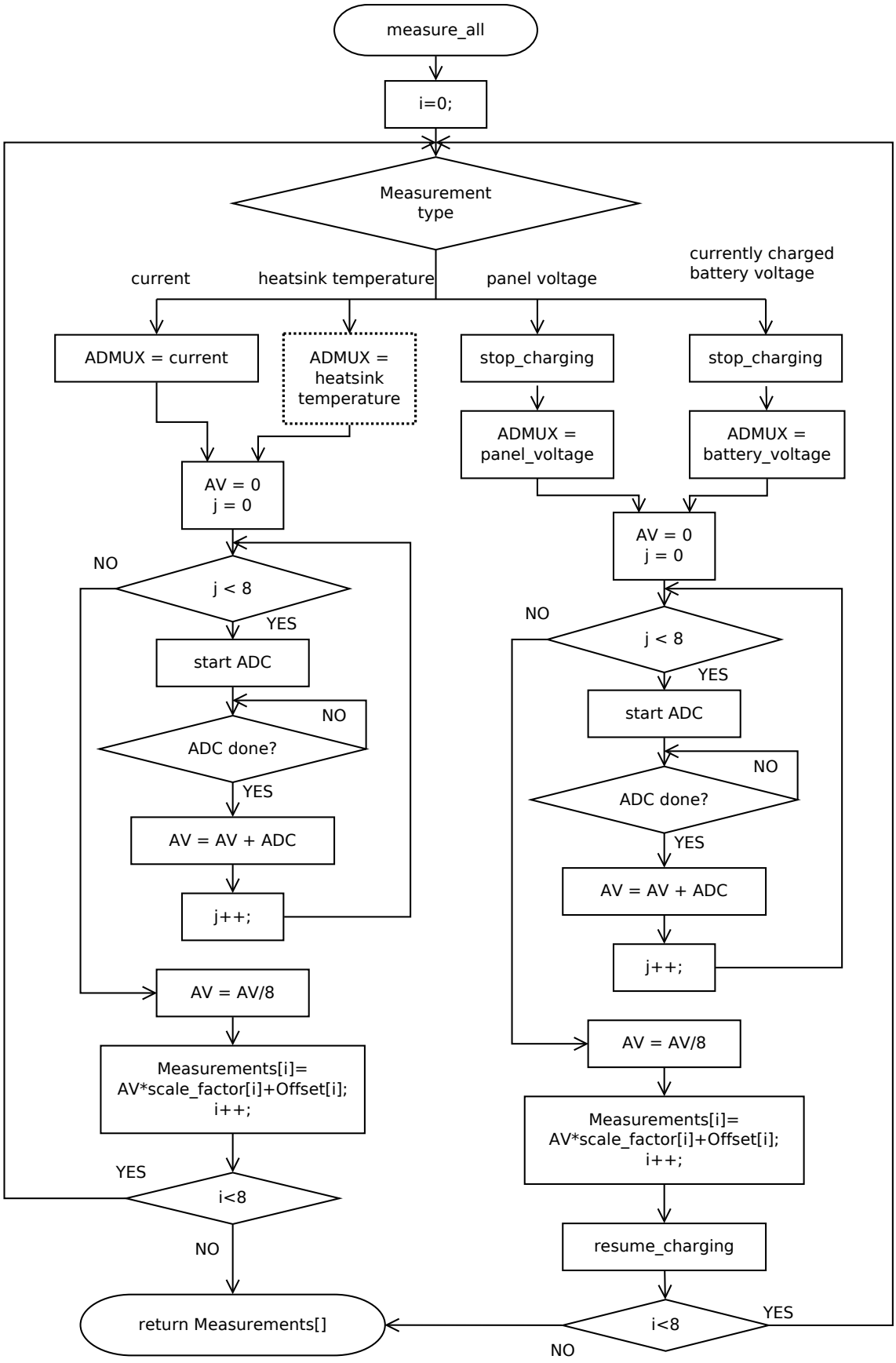

Fig. 3.2: The principle flowchart of *measure_ all()* function

the measurement is finished. This is done in order to get rid of bias caused by fluctuating current. This technique should not affect the amount of energy transferred from the solar panel significantly, as the panel is disconnected only for a fraction of second.

To prevent unnecessarily high effects of noise on measured data, the measurements are carried out several times and the result is averaged. This function also takes care of the necessary scaling of data and adding a previously determined offset value (in case the calibration has been done) to further improve measurement's accuracy.

3.3 Control Logic

The function *control_logic()* is responsible for charging the batteries. It uses data measured previously (voltages and currents through system elements) and decides which battery to connect and whether to connect or disconnect PV panel and load. There are several possible ways how to accomplish this and they are discussed in the following section.

3.3.1 Possible Algorithms

Several algorithms have been considered for choosing the batteries to charge and discharge. Here is their brief description:

Method number 1 This method uses priorities when charging and discharging the batteries. The principle is sketched on diagram in Fig. 3.3a. The batteries on the left are charged first and when they are full the algorithm charges battery that is its neighbour on the right side. When discharging (the current to load is higher than current from solar panel) the algorithm discharges batteries from the right side. There are some advantages and disadvantages of this method:

- The batteries will be fully charged and discharged. This can be useful in isolated solar system where the discharged battery can be removed to be charged outside the system (e.g. from the grid somewhere else).
- Previous fact can be a disadvantage in winter, when the completely discharged batteries can be easily damaged by temperatures below 0°C.
- It would be possible to use algorithm that orders the batteries according to their efficiency and then use this for prioritizing the batteries.

Method number 2 The batteries can be kept as a similar charge level, as it is illustrated in Fig. 3.3b. This can be achieved by switching the batteries more often (e.g. after one minute) and choosing the battery with lowest voltage for charging and highest voltage for discharging.

Method number 3 The batteries can be fully charged in some order and fully discharged in an independent order. The sketch of principle of this method is in Fig. 3.4. Advantage of this method is that every battery will be cycled in time and not left fully charged or fully discharged for long periods of time.

Method number 4 The batteries can be switched periodically for the same fraction of period (e.g. each of 5 batteries for 200ms every second). When charging and some battery is fully charged, it can be removed from the set of batteries being connected and the available time will be redistributed. The same applies to discharging and fully discharged battery.

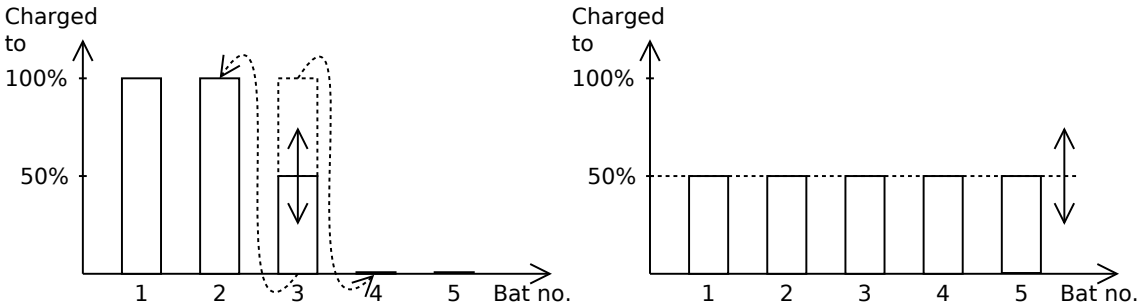

(a) Method no.1 (b) Method no.2

Fig. 3.3: Methods for charging/discharging multiple batteries

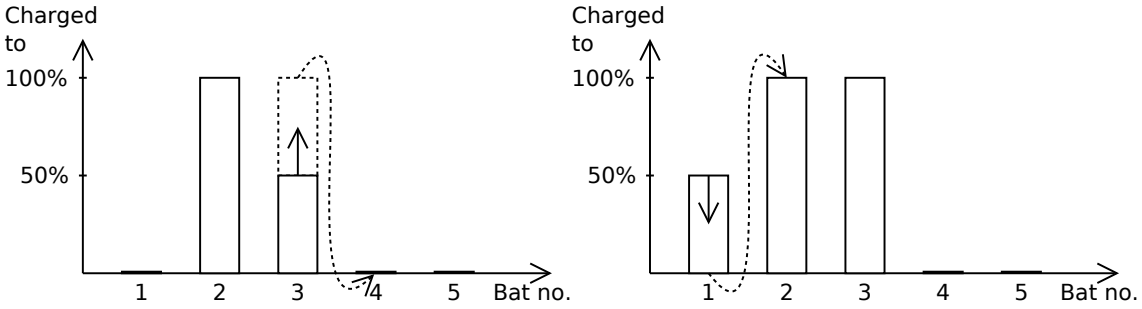

(a) Charging (b) Discharging

Fig. 3.4: Method no.3 for charging/discharging multiple batteries

3.3.2 Implemented Algorithm

The charging method 1 from the previous section has been implemented in the charge controller. It was implemented for 5 batteries which is the maximum number the HW allows.

The functionality is divided into several parts. Function *control_logic()* (its flowchart is shown in Fig. 3.5) uses the measured data (the current from solar panel and current to load) to decide whether the batteries are currently being charged or discharged. Depending on the decision it then runs either the function *choose_bat_for_charging()* or *choose_bat_for_discharging()*. Then the physical outputs of the controller are set using function *control_power_switches()* according to which battery is chosen and whether the panel and load should be connected or not.

This process is followed by a check that shows, if the battery was really charged or really discharged as was determined in the beginning. The reason is that the current sensing can have an error in measurement of 2% when calibrated and up to 14% without calibration. Wrong information about charging or discharging could cause the algorithm of method 1 to fail which is prevented by the above mentioned check.

Function *choose_bat_for_discharging()* (its flowchart can be seen in Fig. 3.6) was designed so that it ignores the battery inputs where no batteries are connected and the batteries that have too low voltage and are therefore presumed to be damaged. After it identifies battery to connect it also decides if the solar panel is able to recharge the battery. This prevents the solar panel from discharging the batteries at night.

Similar principle is used in *choose_bat_for_charging()* function (its flowchart is divided into 2 parts in Fig. 3.7 and Fig. 3.8). However, this implementation charges batteries in two phases. Firstly it is possible to charge them all to a certain threshold, only then they are charged to 100%.

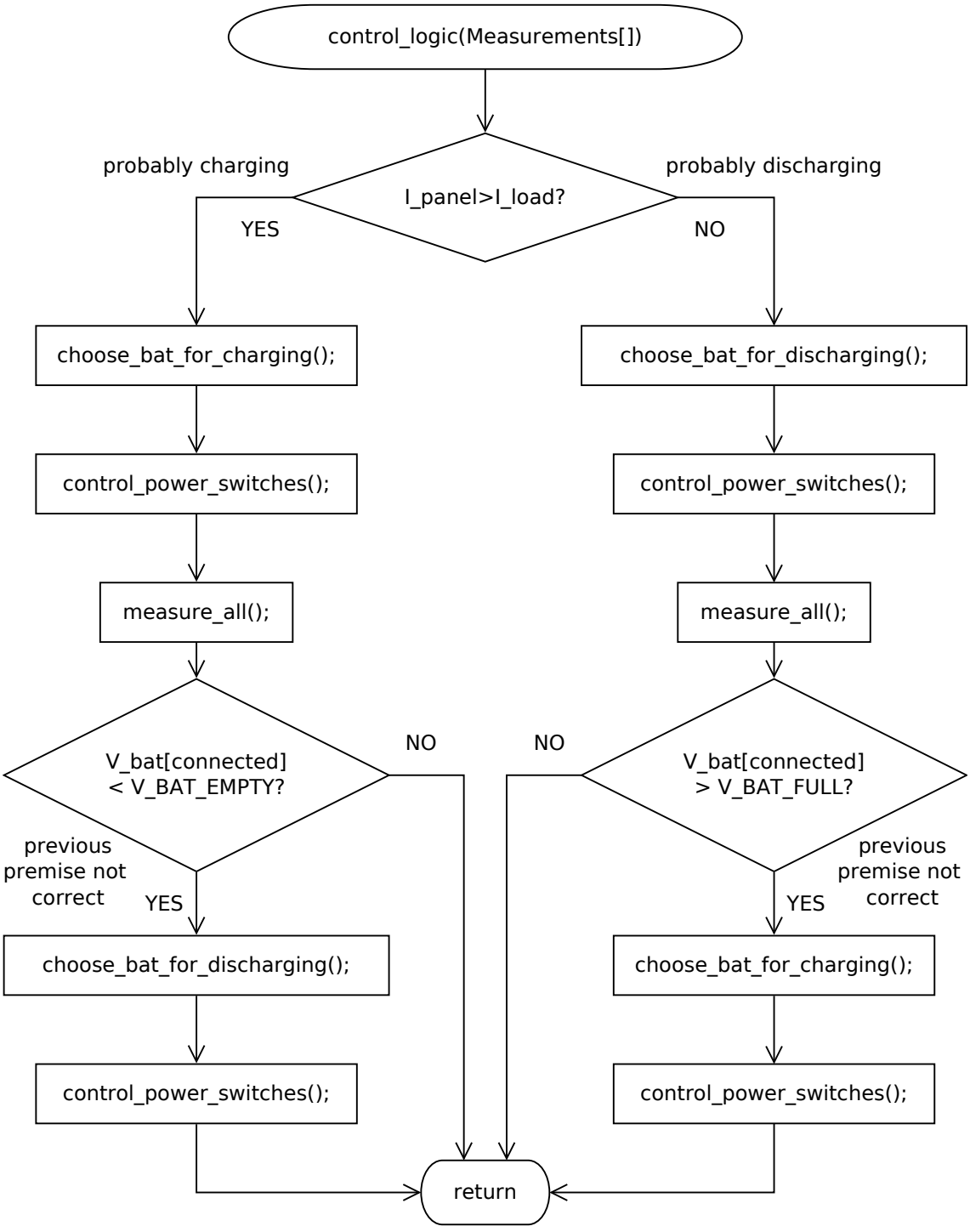

Fig. 3.5: The principle flowchart of *control_ logic()* function

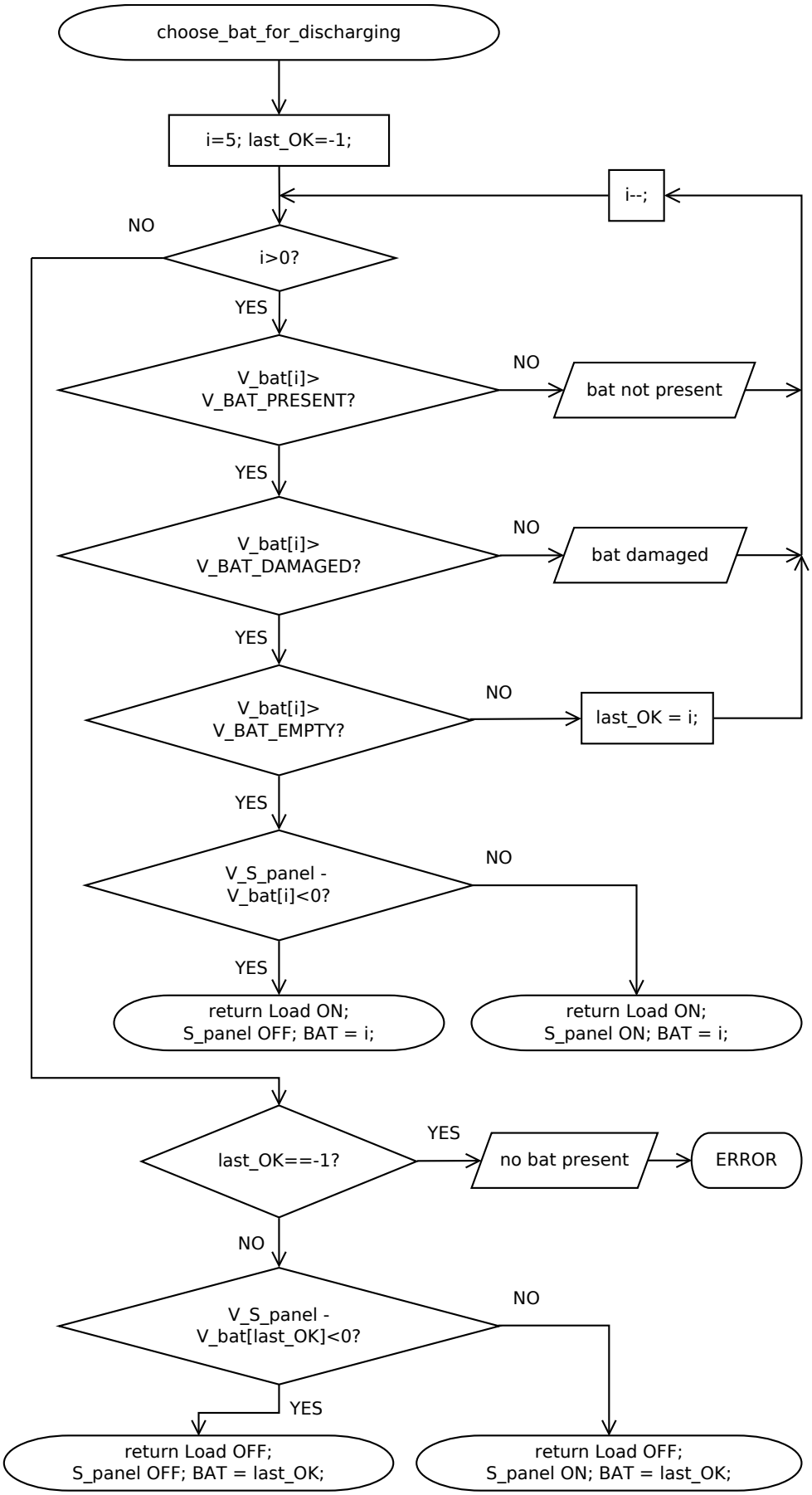

Fig. 3.6: The flowchart of *choose_ bat_ for_ discharging()* function

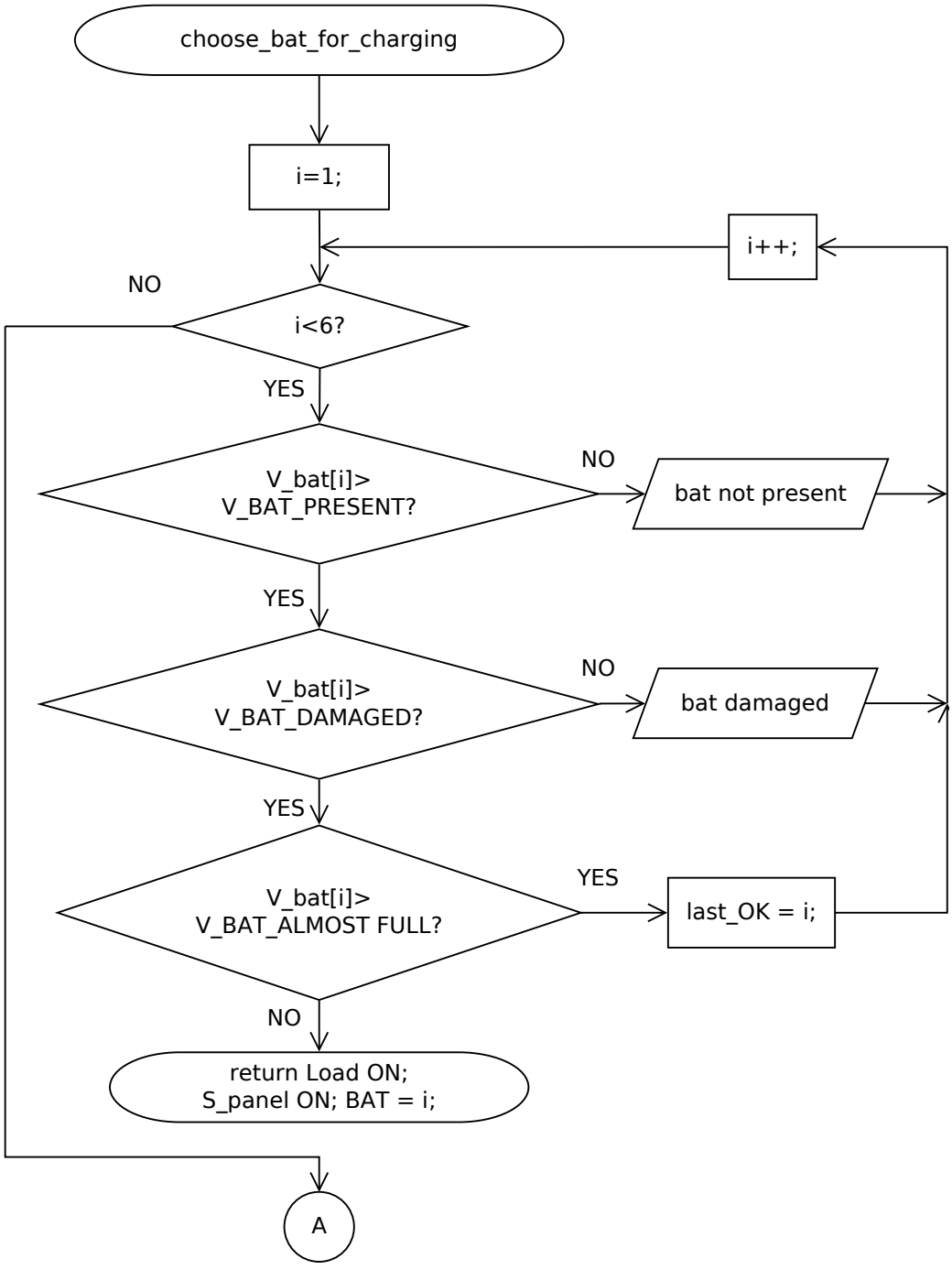

Fig. 3.7: The flowchart of *choose_ bat_ for_ charging()* function – part 1

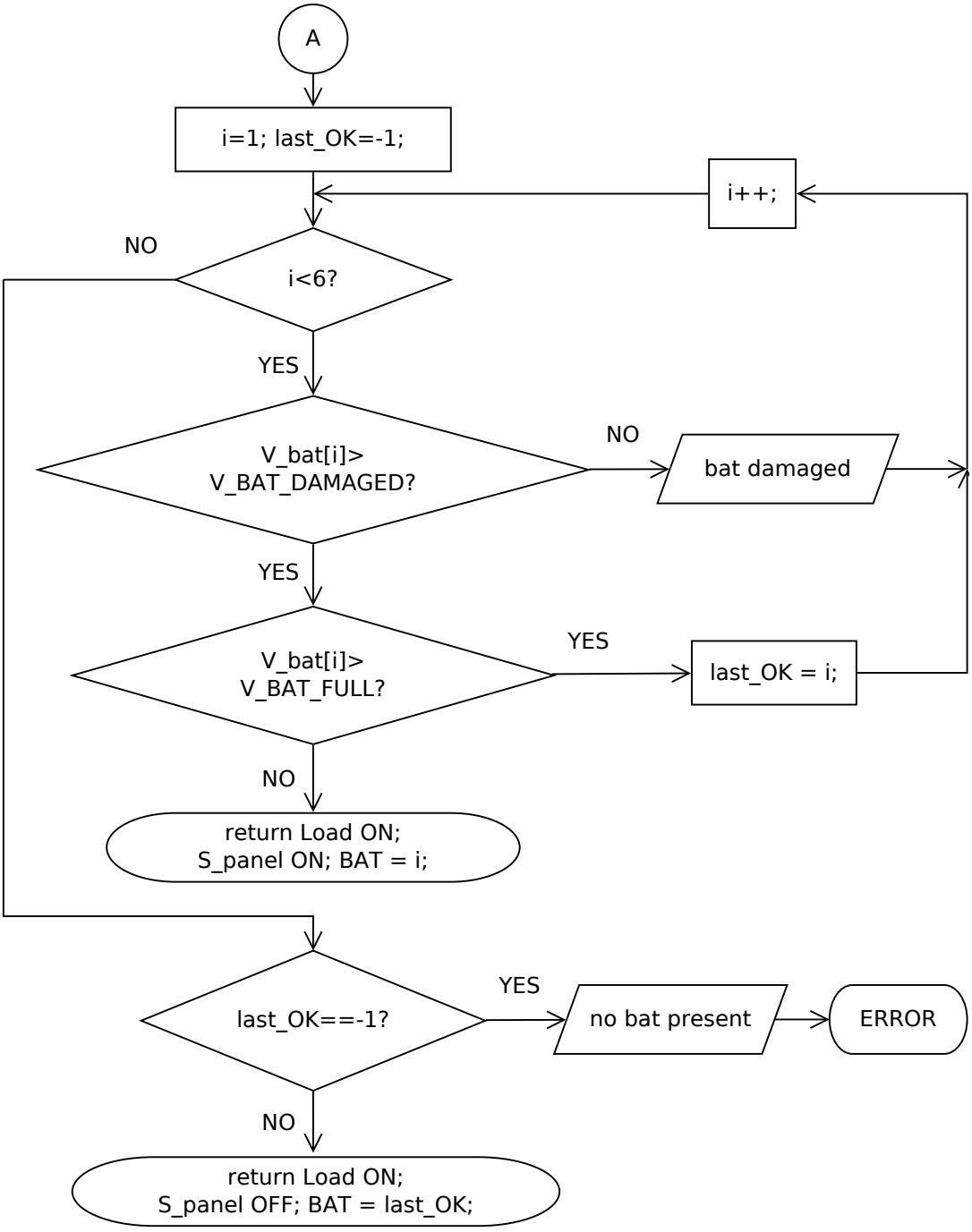

Fig. 3.8: The flowchart of *choose_ bat_ for_ charging()* function – part 2

4 MEASUREMENTS ON PROTOTYPE

The correct functionality of the charge regulator has been verified by two means:

- by verifying the correct functionality under multiple scenarios using external voltmeters on the batteries,
- and by sending the measured data and information about controller's current output to PC.

The results of the second method of verification will be described in the following sections.

4.1 Method of Measurement

As was already mentioned, the measurement was automatized to a great extent. The software for the controller contains a mechanism for sending error messages, measurement results and information about its state to the outer world via UART. This output was then fed to MAX232 RS-232 driver/receiver circuit for changing the voltage levels so that a communication with PC could be established.

The data was received by the PC using software called Realterm [38]. It offers a possibility to save the incoming data from a serial port directly to file. This possibility was used to save the vital information during simulation of different scenarios the controller should be able to handle (the actions applied during the simulation are listed in Table 4.1). This data was then subjected to analysis and presentation of results, which follows in the next section.

Tab. 4.1: Simulated scenarios and their occurence in time

Time [s]	Action
0	Only battery no. 2 is connected
5	Battery no. 1 is connected
12	21W light bulb (load) is connected
20	Source of power for charging is connected
30	Load is disconnected
40	Battery no. 2 is disconnected
47	5W light bulb is connected

In order to make the information about measurement complete, the values of constants used in the function responsible for charging (described in Section 3.3.2) are listed in 4.2. Note that these values are experimental and can be changed before

applying the controller in real life. Moreover, it has to be stated that the battery number 1 used for the measurements was Panasonic rechargeable sealed lead-acid battery with capacity 2.2Ah and battery number 2 was also sealed lead-acid battery with 26.7Ah capacity. It was also found that the period of 1s of the implemented software is too long for batteries with small capacity, such as battery no. 1 used for measurements. But as the charge controller is designed for batteries with tens or hundreds of Ah, this time constant does not have to be changed.

Tab. 4.2: Values of several constants used in *control_logic()* function

Constant	Value [V]
V_BAT_PRESENT	4.0
V_BAT_DAMAGED	9.0
V_BAT_EMPTY	10.5
V_BAT_ALMOST_FULL	13.5
V_BAT_FULL	13.8

4.2 Results

Data acquired by the measurement during above mentioned simulation are plotted in Fig. 4.1. Note that the inputs for other batteries have not been used and the corresponding voltages are not plotted in the graphs, because the increased number of data inputs would make the analysis very complicated and results much harder to be plotted clearly. The logical output of the controller for switching the load is not shown either, as it keeps value of logical 1 for the whole length of measurement.

Let the behaviour of the controller in response to simulated actions be described for the individual intervals:

0–5s – battery number 2 is connected by the controller, which is the desired behaviour as it is the only one available,

5–12s – battery number 2 stays connected, because there is no charging available, so a charged battery with the highest number should be connected,

12–20s – the load is discharging battery no. 2 and its voltage is slowly decreasing,

20–30s – as the charging current is bigger than current to load, so the controller switches to battery no. 1, as it is not full and therefore should be preferred for charging,

30–40s – the charging current is quite high and the controller switches between batteries 1 and 2, because the voltage of battery number one rises above and falls

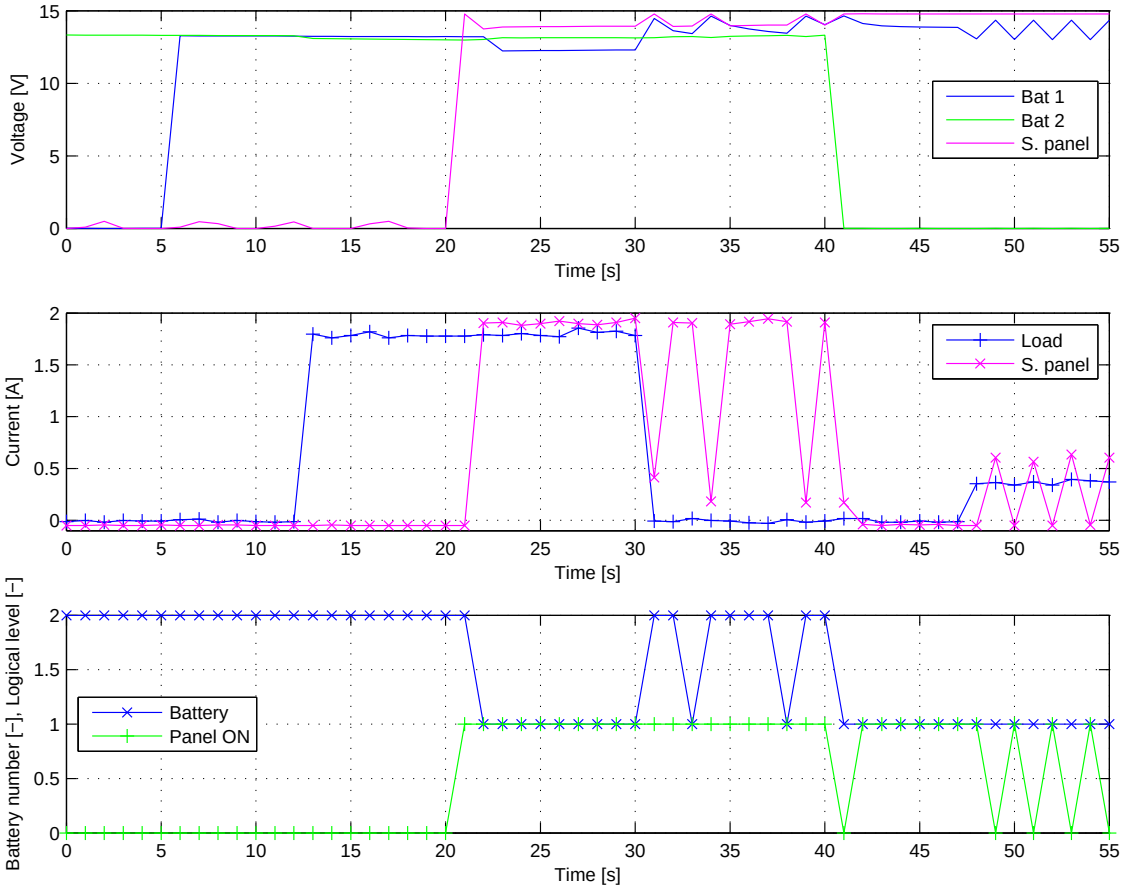

Fig. 4.1: Graphs of the measured data

below the threshold for full battery repeatedly. The charging current oscillates between high value for battery 2 and smaller value for battery 1 because of their different capacity and state of charge,

40–47s – as battery 1 is the only one left, it is connected and being charged,

48–55s – the charger keeps switching the charging on and off, because the voltage of battery keeps rising above and falling below the threshold for full battery.

Performed simulation of basic events that the controller should handle correctly has shown that:

- controller is able to respond correctly to connecting and disconnecting the batteries,
- controller is able to connect the batteries as expected (according to implemented charging method number 1),
- input for solar panel is disconnected when it is not able to supply power, and
- current measurement is working as expected (e.g. measured current is proportional to load power input).

CONCLUSION

The purpose of this thesis was to design and implement a charge controller for charging multiple lead-acid batteries. In order to be able to charge the batteries correctly and effectively, the methods of charging lead-acid batteries, the related issues and the specifics of photovoltaic applications have been studied in literature.

With the use of this knowledge a list of desirable features of new controller has been formulated. These features were subjected to a review and most of them were chosen to be implemented in the design of the regulator. In the following phase a block diagram of the proposed charge controller has been forged, such that the final product could incorporate all the chosen functionality.

Then the detailed requirements for all of the blocks of proposed block diagram have been specified. The following design phase accompanied by test implementation of the most complicated units, such as power switches and current measurement circuits, led to improvements and modifications to the preliminary block diagram and the design of these blocks.

Because the design was aimed for as many batteries as possible, the resulting schematic diagram for the whole controller contained too many parts. Moreover, the connections were of very different character (high power ones for currents of 20A and the rest for logic with currents in the order of only mA). This would have made the hardware implementation on a single printed circuit board very impractical. That is why the design was decomposed into two logical parts – Logic Board and Power Board.

After finishing the design of the whole system, the prototype implementation of the charge controller has been produced. This consisted of securing correct design and production of Printed Circuit Boards, procurement of the necessary parts, soldering these parts into the board, fitting the product into the case, and overcoming problems that arose during this process.

One of several control algorithms that have been devised for correct charging and discharging of multiple batteries has been implemented using this hardware. This was followed by a verification of correct behaviour of implemented hardware and software elements by measurements.

Here is a list of features incorporated and tested in the current version of the charge controller:

- as many as 5 terminals for batteries designed for as much as 20A of nominal current,
- connection and disconnection of the batteries is automatically recognized by the controller and they are used by the controller as long as they are not damaged,

- short circuit protection – short circuiting the output does not result in damage of the hardware,
- ability to send data to PC via serial connection,
- protection against reverse battery connection,
- thermal protection,
- protection of inputs against transient voltages using Transient Voltage Suppressor diodes,
- practical design that offers convenient connection of thick cables from the batteries.

The future work on improving this charge controller can concentrate on implementing and tuning more algorithms for charging and discharging multiple batteries that have been devised in this work and on comparing their benefits in various situations. The planned detached units of the controller for data logging and remote user interface can be designed and implemented as well. Moreover, the controller has been designed for additional features that could be easily implemented and tested during subsequent work:

- data logging,
- over-current protection,
- protected RS-485 interface with fail safe bias,
- battery and ambient temperature measurement,
- battery performance analysis and battery condition monitoring and display (thanks to measurement of vital information such as voltage and current, and to possibility to measure battery temperature).

Even though the design of this controller was rather time consuming, the investments into this technology should be returned with more economical battery management in an isolated solar system and better utilization of potentially environmentally dangerous lead-acid batteries.

BIBLIOGRAPHY

[1] HOROWITZ, Paul; HILL, Winfield. *The Art of Electronics*. Second Edition. Cambridge (United Kingdom) : Cambridge University Press, 1989. xxiii, 1125 s. ISBN 0 521 37095 7.

[2] BOLDIŠ, P. *Bibliografické citace dokumentů podle ČSN ISO 690 a ČSN ISO 690-2* [online]. 2001, last revision 11. 11. 2004 [cit. 2011-07-19]. URL: <http://www.boldis.cz/citace/citace.html>.

[3] KMa Webdesign. *Citace 2.0 : vše o citování literatury a dokumentů* [online]. Citace.com, c2009, last revision July 19, 2011 [cit. 2011-07-19]. Generátor citací. URL: <http://citace.com/generator.php>.

[4] *Konarka Power Plastic* [online]. c2011, last revision July 19, 2011 [cit. 2011-07-19]. URL: <http://www.konarka.com/>.

[5] *Wikipedia : the free encyclopedia* [online]. 2010, last modified on 6 July 2011 [cit. 2011-07-19]. Lead–acid battery. URL: <http://en.wikipedia.org/wiki/Lead-acid_battery>.

[6] *Using the bq2031 to Charge Lead-Acid Batteries* [online]. c1999 [cit. 2011-07-19]. Unitrode Application note U-510. URL: <http://www.nalanda.nitc.ac.in/industry/appnotes/Texas/analog/slua017.pdf>.

[7] CHERNG, J.Y. – KLANG, J.K. *Method for optimizing the charging of lead-acid batteries and an interactive charger* [online]. Nov. 21, 1995 [cit. 2011-07-19]. Google Patents - US Patent 5,469,043.

[8] ANDERSON, E. – DOHAN, C. – SIKORA, A. *Solar Panel Peak Power Tracking System.*Worcester, 2003. 166 pages. Major Qualifying Project. Worcester Polytechnic Institute. URL: <http://ece.wpi.edu/analog/mqps/SolarMQP.pdf>. Project Number: MQP-SJB-1A03.

[9] STORR, Wayne *Electronics-Tutorials* [online]. c1999-2011, last revision June 27, 2011 [cit. 2011-07-20]. Using the Power MOSFET as a Switch. URL: <http://www.electronics-tutorials.ws/transistor/tran_7.html>.

[10] *High-Side Current-Sense Measurement: Circuits and Principles* [online]. Nov 19, 2001, last revision 3/16/2011 [cit. 2011-07-21]. Maxim Application note 746. URL: <http://pdfserv.maxim-ic.com/en/an/AN746.pdf>.

[11] *Allegro MicroSystems, Inc. : High-Performance Power and Hall-Effect Sensor ICs* [online]. c2011, last revision July 21, 2011 [cit. 2011-07-21]. Current Sensor ICs. URL: <http://www.allegromicro.com/en/Products/Categories/Sensors/currentsensor.asp>.

[12] *Asahi Kasei : Asahi Kasei Microdevices Corporation* [online]. Last revision June 23, 2010 [cit. 2011-07-21]. Current sensor. URL: <http://www.asahi-kasei.co.jp/ake/en/product/current_sensor/index.html>.

[13] *CSLA2CD* [online]. c2004, last revision 4/14/2006 [cit. 2011-07-21]. Honeywell Datasheet. URL: <http://catalog.compel.ru/dat/sensor_current/HONEY/pdf/CSLA2CD.pdf>.

[14] *CSNE151* [online]. c2006, last revision 8/31/2006 [cit. 2011-07-21]. Honeywell Datasheet. URL: <http://catalog.compel.ru/file/sensor_current/HONEY/pdf/CSNE151.pdf>.

[15] *IR3313(S)PbF: Programmable Current Sense High Side Switch* [online]. Last revision 10/3/2010 [cit. 2011-07-21]. International Rectifier Data Sheet No. PD60288_D. URL: <http://www.irf.com/product-info/datasheets/data/ir3313pbf.pdf>.

[16] JACQUINOD, David. *IR331x : Current Sensing High Side Switch – P3* [online]. 2007, last revision 4/2/2008 [cit. 2011-07-21]. International Rectifier Application Note AN- 1118. URL: <http://www.irf.com/technical-info/appnotes/an-1118.pdf>.

[17] *IRF3205: HEXFET®Power MOSFET* [online]. 01/25/01, last revision 08/18/2007 [cit. 2011-07-25]. International Rectifier Data Sheet PD-91279E. URL: <http://www.irf.com/product-info/datasheets/data/irf3205.pdf>.

[18] *Wikipedia : the free encyclopedia* [online]. 2007, last revision: 25 January 2011 [cit. 2011-07-22]. Float voltage. URL: <http://en.wikipedia.org/wiki/Float_voltage>.

[19] *AVR450: Battery Charger for SLA, NiCd, NiMH and Li-Ion Batteries* [online]. c2006, last revision 11/16/2006 [cit. 2011-07-22]. Atmel Corporation Application Note AVR450. URL: <http://www.atmel.com/dyn/resources/prod_documents/doc1659.pdf>.

[20] *LM4040 - Precision Micropower Shunt Voltage Reference* [online]. December 9, 2010 [cit. 2011-07-22]. National Semiconductor Data Sheet. URL: <http://www.national.com/ds/LM/LM4040.pdf>.

[21] *AVR521: Migrating from ATmega32 to ATmega32A* [online]. c2008, Rev. 8162A-AVR-06/08 [cit. 2011-07-23]. Atmel Corporation Application Note AVR450. URL: <http://atmel.com/dyn/resources/prod_documents/doc8162.pdf>.

[22] *ATmega32A* [online]. c2011, last revision 2/28/2011 [cit. 2011-07-23]. Atmel Corporation Data Sheet. URL: <http://www.atmel.com/dyn/resources/prod_documents/doc8155.pdf>.

[23] *Atmel AVR042: AVR Hardware Design Considerations* [online]. c2011, Rev. 2521K-AVR-03/11 [cit. 2011-07-23]. Atmel Corporation Application Note AVR042. URL: <http://www.atmel.com/dyn/resources/prod_documents/doc2521.pdf>.

[24] *LE00AB/C series: Very low drop voltage regulators with inhibit* [online]. August 2003 [cit. 2011-07-23]. STMicroelectronics Data Sheet. URL: <http://i2c2p.twibright.com/datasheet/LE00AB_regulator.pdf>.

[25] *World Products, LLC : Electronic Equipment Solutions* [online]. c2011, last revision January 26, 2011 [cit. 2011-07-23]. Transient Voltage Suppression Diodes - General Information. URL: <http://www.worldproducts.com/TVSDiodesGenInfo.htm>.

[26] *LM135/LM235/LM335, LM135A/LM235A/LM335A Precision Temperature Sensors* [online]. December 17, 2008 [cit. 2011-07-23]. National Semiconductor Data Sheet. URL: <http://www.national.com/ds/LM/LM135.pdf>.

[27] *ATM1602B Liquid Crystal Display Module* [online]. 11/7/2003, last revision 11/5/2011 [cit. 2011-07-23]. URL: <http://www.gme.cz/_dokumentace/dokumenty/513/513-128/dsh.513-128.1.pdf>.

[28] *DS18B20 Programmable Resolution 1-Wire Digital Thermometer* [online]. c2008, last revision 2/15/2011, REV:042208 [cit. 2011-07-23]. Maxim Integrated Products Data Sheet. URL: <http://datasheets.maxim-ic.com/en/ds/DS18B20.pdf>.

[29] KUGELSTADT, T. *Protecting RS-485 Interfaces Against Lethal Electrical Transients* [online]. May 2009, Revised March 2011 [cit. 2011-07-23]. Texas Instruments Application Report SLLA292A. URL: <http://focus.ti.com/lit/an/slla292a/slla292a.pdf>.

[30] MARAIS, H. *RS-485/RS-422 Circuit Implementation Guide* [online]. c2008 [cit. 2011-07-23]. Analog Devices Application Note AN-960. URL: <http://www.analog.com/static/imported-files/application_notes/AN-960.pdf>.

[31] KUGELSTADT, T. *Isolated RS-485 Reference Design* [online]. October 2009 [cit. 2011-07-23]. Texas Instruments Application Report SLLA299. URL: <http://focus.tij.co.jp/jp/lit/an/slla299/slla299.pdf>.

[32] *Low-Power, Slew-Rate-Limited RS-485/RS-422 Transceivers* [online]. c2009, Rev 9, 9/09 [cit. 2011-07-23]. Maxim Integrated Products Data Sheet. URL: <http://datasheets.maxim-ic.com/en/ds/MAX1487-MAX491.pdf>.

[33] ŘÍHA, Z. *Zásady používání RS485* [online]. 4.8.2010, last revision 7.5.2010 [cit. 2011-07-23]. AMiT Application Note AP0016. URL: <http://amitomation.cz/support/cz/aplikacni_poznamky/ap0016_cz_02.pdf>.

[34] *Thermal Management Using Heat Sinks* [online]. March 2002, last revision 9/2/2003, ver. 2.1 [cit. 2011-07-25]. Altera Corporation Application Note 185. URL: <http://www.altera.com/literature/an/archives/an185.pdf>.

[35] *Daycounter, Inc. : Engineering Services* [online]. c2004, last revision July 25, 2011 [cit. 2011-07-25]. Heat Sink Temperature Calculator. URL: <http://www.daycounter.com/Calculators/Heat-Sink-Temperature-Calculator.phtml>.

[36] *Multi Circuit Boards: Printed Circuit Board Prototypes and Series* [online]. Last revision July 26, 2011 [cit. 2011-07-26]. Conductor / Ampacity. URL: <http://www.multi-circuit-boards.eu/en/pcb-design-aid/design-parameters/conductor-ampacity.html>.

[37] *The CircuitCalculator.com Blog: a blog with live web calculators* [online]. January 31, 2006, last revision July 26, 2011 [cit. 2011-07-26]. PCB Trace Width Calculator. URL: <http://circuitcalculator.com/wordpress/2006/01/31/pcb-trace-width-calculator/>.

[38] *RealTerm: Serial/TCP Terminal* [PC program]. Ver. 2.0.0.57. c1987-2008 [cit. 2011-07-27]. URL: <http://realterm.sourceforge.net/index.html>.

[39] WENTZEL, C. *vonWentzel.net* [online]. c1997, Latest update on January 22, 2008 [cit. 2011-07-28]. How Lead Acid Batteries Work. URL: <http://www.vonwentzel.net/Battery/00.Glossary/>.

[40] *Improved charging methods for lead-acid batteries using the UC3906* [online]. c1999 [cit. 2011-07-28]. Unitrode Application note U-104. URL: <http://focus.ti.com/lit/an/slua115/slua115.pdf>.

[41] BUCHMANN, I. *Battery University* [online]. c2011, last revision July 29, 2011 [cit. 2011-07-29]. Charging Lead Acid. URL: <http://batteryuniversity.com/learn/article/ charging_the_lead_acid_battery>.

LIST OF SYMBOLS, PHYSICAL CONSTANTS AND ABBREVIATIONS

PV photovoltaic

LCD Liquid Crystal Display

LED Light-Emitting Diode

TVS Transient Voltage Suppressor

µC microcontroller

PC personal computer

ADC Analog to Digital Converter

HW hardware

SW software

PCB Printed Circuit Board

SSR Solid State Relay

MOSFET Metal-Oxide-Semiconductor Field-Effect Transistor

PWM Pulse-Width Modulation

$R_{DS(on)}$ static drain-to-source on-resistance

V_{GS} gate-to-source voltage

V_{DSS} drain-to-source voltage

I_D continuous drain current

AN Application Note

IC Integrated Circuit

I_Q quiescent current

I_L load current

R_S series resistance

R_{REF} resistance of reference input

DIL dual in line

SMD Surface Mount Device

UART Universal Asynchronous Receiver/Transmitter

ESD electrostatic discharge

TVS Transient Voltage Suppressor

I/O Input/Output

SPI Serial Peripheral Interface

I^2C Inter-Integrated Circuit, also called "two-wire interface"

HIU Human Interface Unit

UTP Unshielded Twisted Pair

STP Shielded Twisted Pair

Θ_{JA} junction-to-ambient thermal resistance

Θ_{CA} case-to-ambient thermal resistance

Θ_{JC} junction-to-case thermal resistance

Θ_{CS} case-to-heat sink thermal resistance

Θ_{SA} heat sink-to-ambient thermal resistance

T_J junction temperature

T_A ambient temperature

P power

LIST OF APPENDICES

A CD WITH SOFTWARE AND THIS DOCUMENT

The CD supplied with this thesis contains the software developed for the implemented charge controller, snapshot of the online resources cited above as well as an electronic version of this document.

B SCHEMATIC DIAGRAM OF POWER BOARD

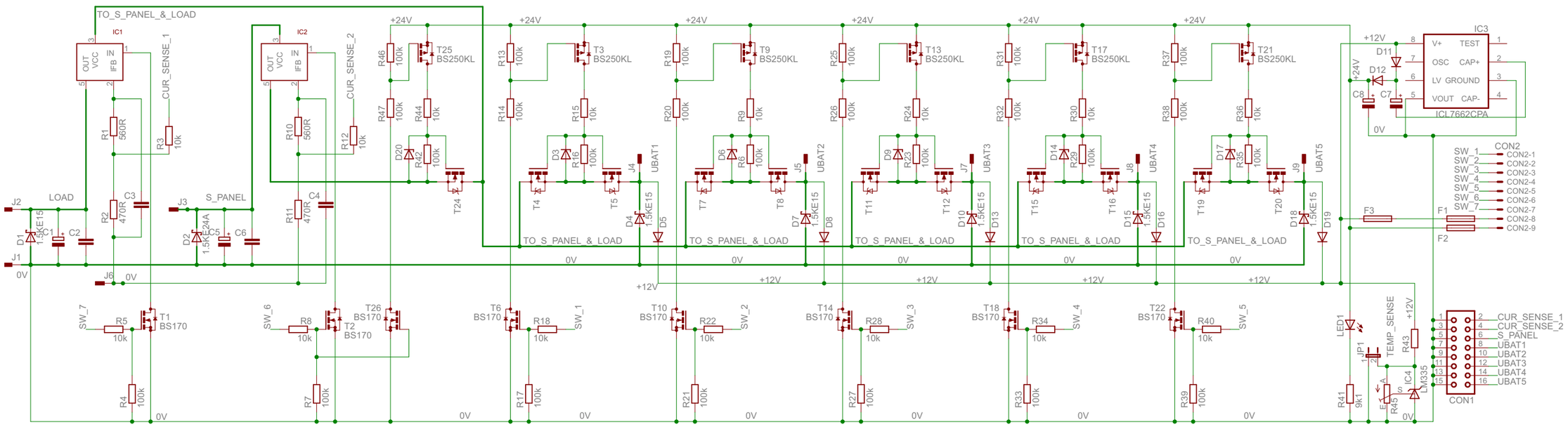

Fig. B.1: Schematic diagram of the Power Board

C SCHEMATIC DIAGRAM OF LOGIC BOARD

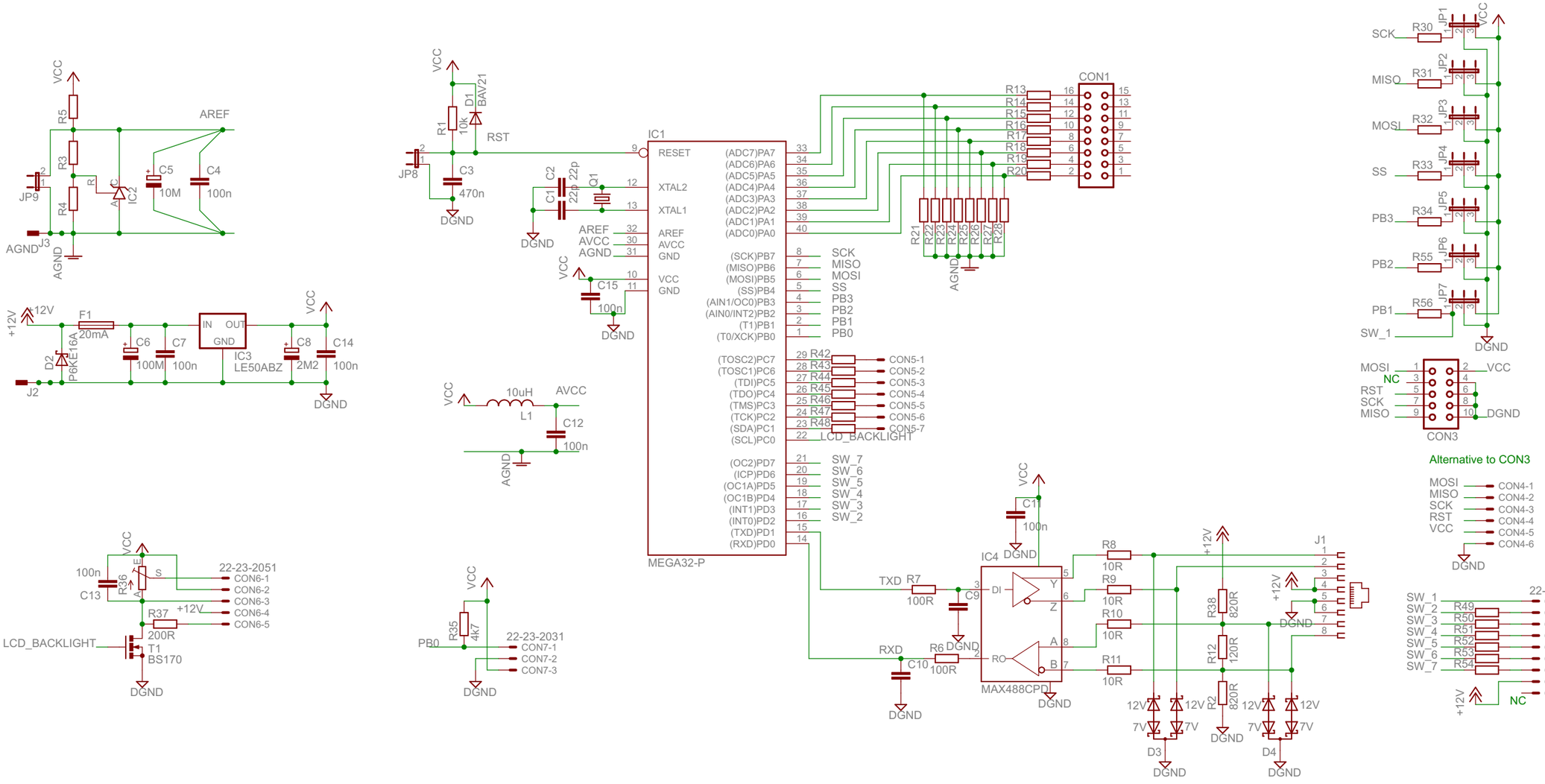

Fig. C.1: Schematic diagram of the Logic Board